IR Echo and New Dust in SN2023ixf: An Optical/NIR Portrait of a hydrogen-rich supernova

Multi-Messenger Astrophysics in the Dynamic Universe,
YITP Workshop Week 4

Avinash Singh
Post-Doctoral Researcher, The Oskar Klein Centre, SU

Introduction

Mass-loss in Massive Stars

Mass-loss is extremely important:
- in understanding how the star evolves
- Explosion as type of supernovae
- Whether it forms a neutron star or a black hole

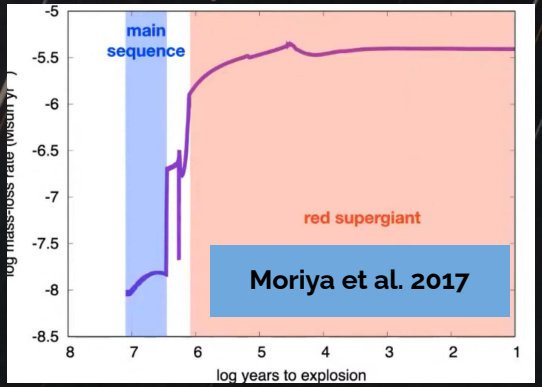

Mass-loss is enhanced in the years prior to explosion - as a RSG

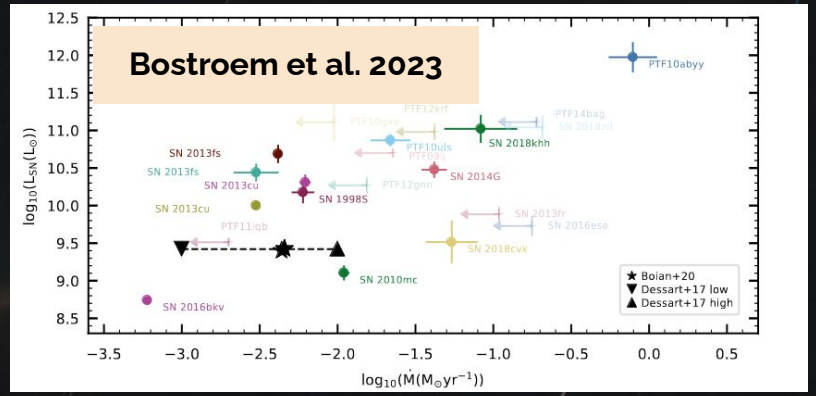

Steady mass-loss mechanisms not enough to explain the dense confined mass near Type II SN

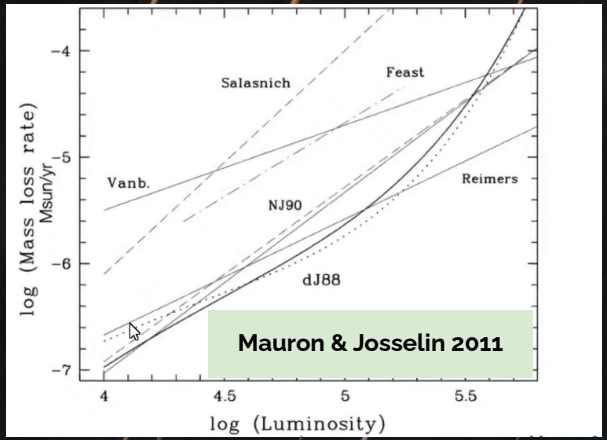

Steady state RSG mass-loss rates are uncertain

Mass-Loss in RSGs shows up as Circumstellar matter in Type II SNe

Early we detect a SN

Closer we get to probing the end Stages of mass-loss in massive stars

SN2023ixf : A once in a decade supernova

Hosseinzadeh+ 2023

Nearby Host : M101 (6.8 Mpc)

Discovered within 27 hours of the explosion

High Cadence follow-up data from Far-UV to the NIR/MIR Wavelengths

Why is 2023ixf special?

Perley+ 2023

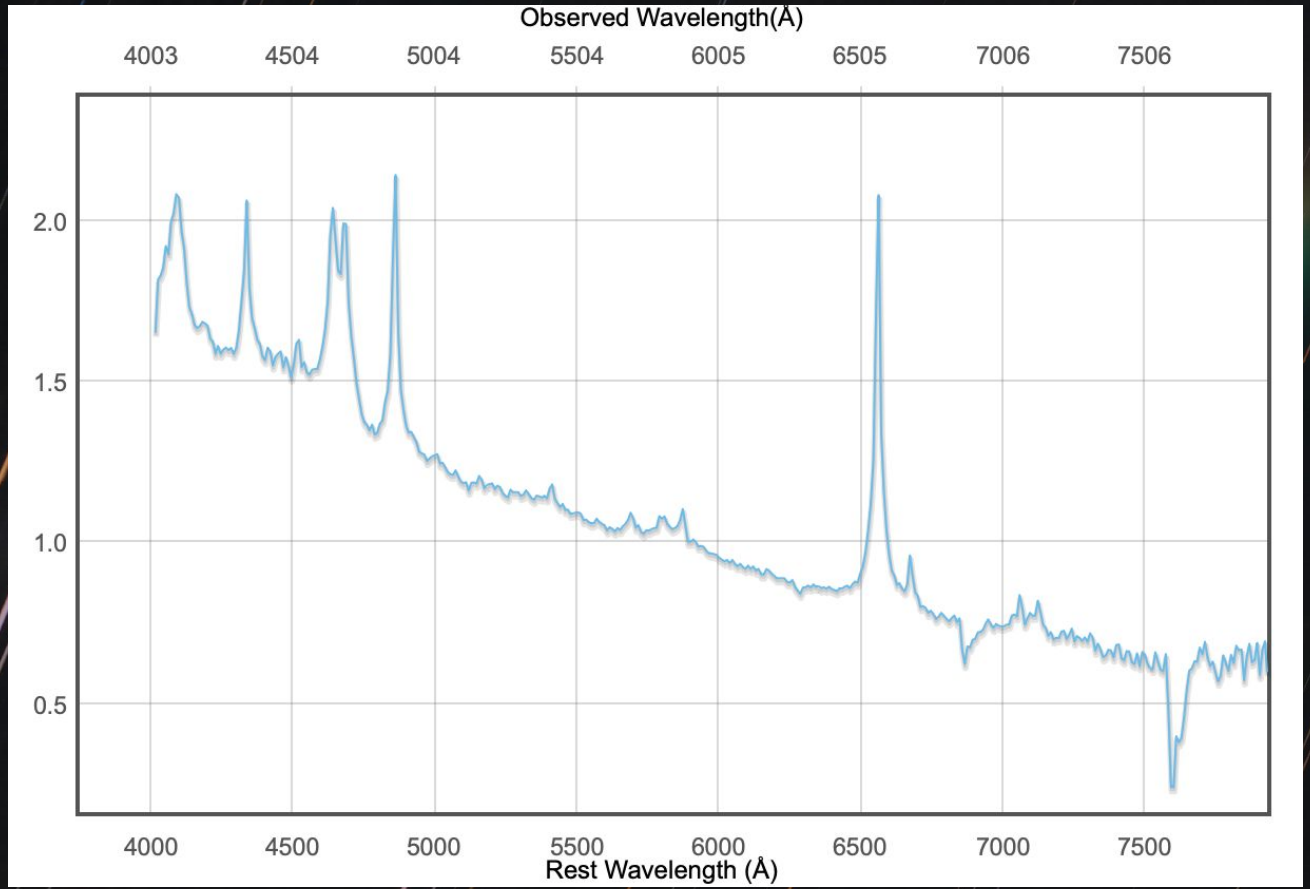

Early Flash-Ionized Features

C IV 1550, He II 1640, and N III] 1750
Si IV 1400, Ni II

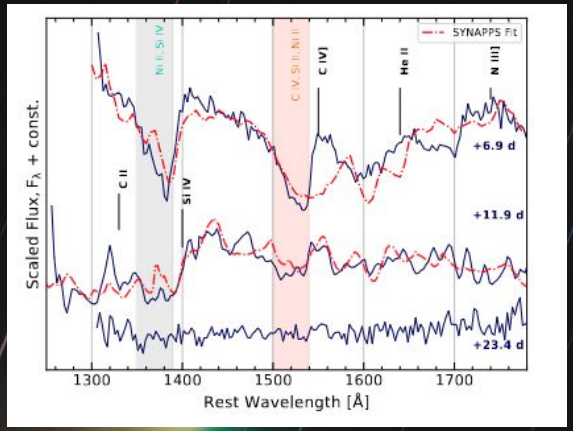

80+ Papers out on arXiv

Grefenstette+2023

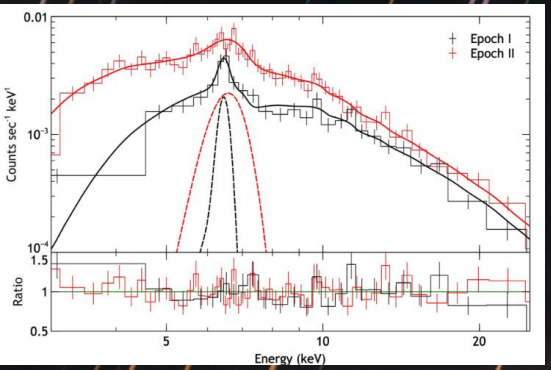

Smith+ 2023

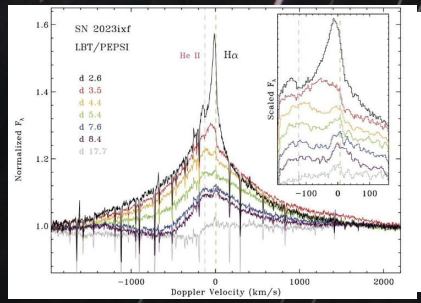

Bostroem+ 2023

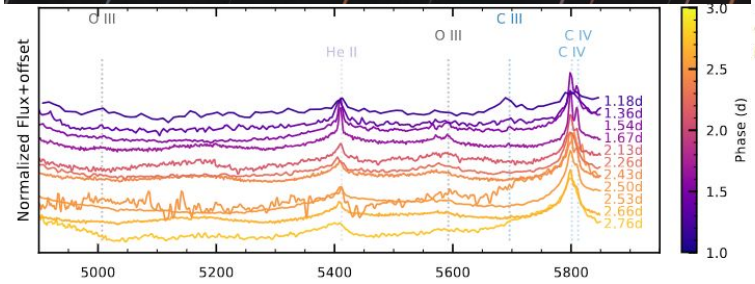

Jacobson-Galan+ 2023

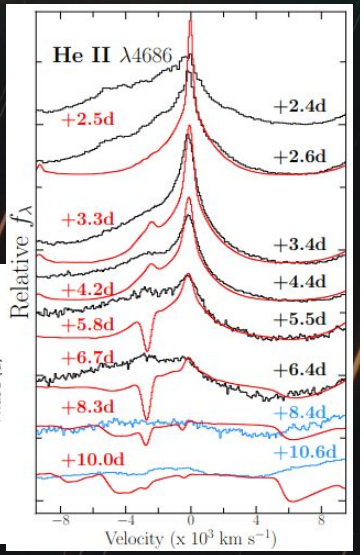

Teja, Singh+ 2023

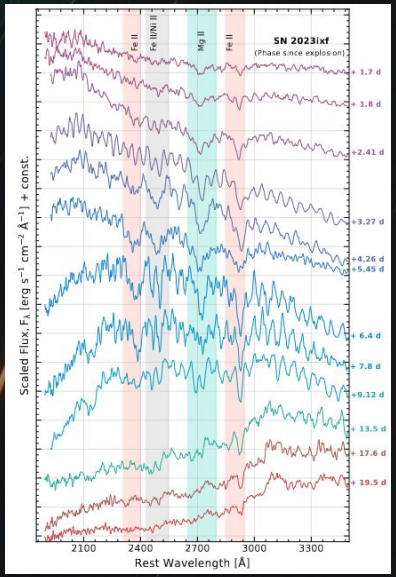

Delayed Shock Breakout

- Delayed Shock Breakout inside a dense CSM.
- Rapid rise in Temperature
- Rapid rise in UV fluxes (Color)
- (nearly)-flat radius evolution
- UVW1-V color also shows the migration towards bluer color

Comparison in UV with other Type IIP/L SNe

- Bol LC rises 15 times from SWIFT detection at 1.5 d (Similar to NUV flux rising 15 times.)
- One of the bluest Type IIP/L SN ever
- There a rise in the flux of the ionized lines up to 4d - Indicating heating of the ejecta.

Singh+24

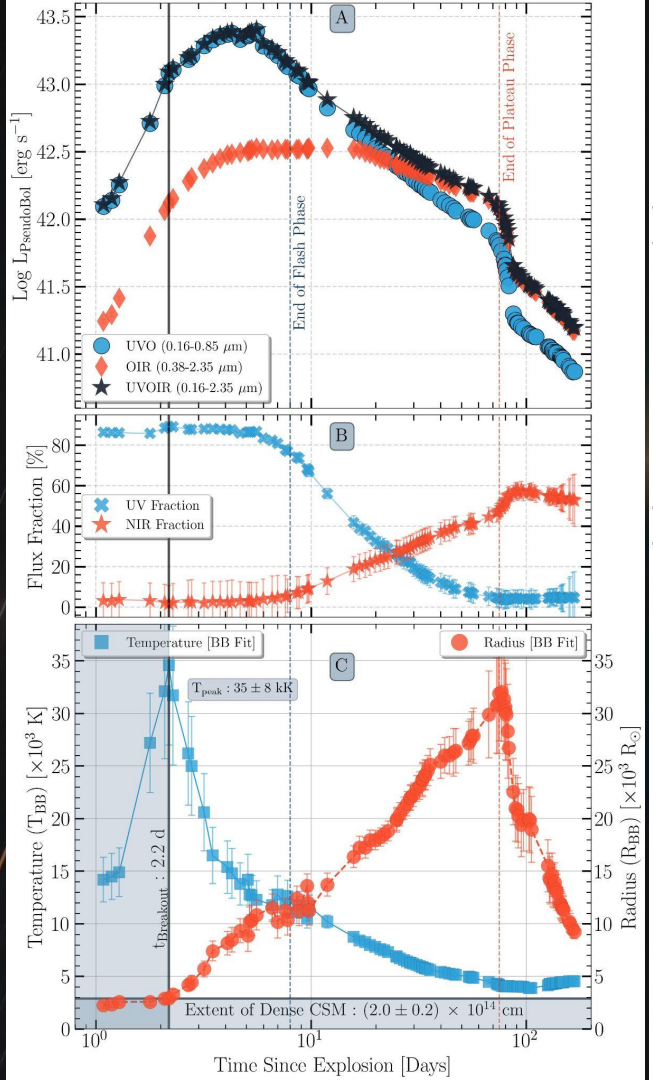

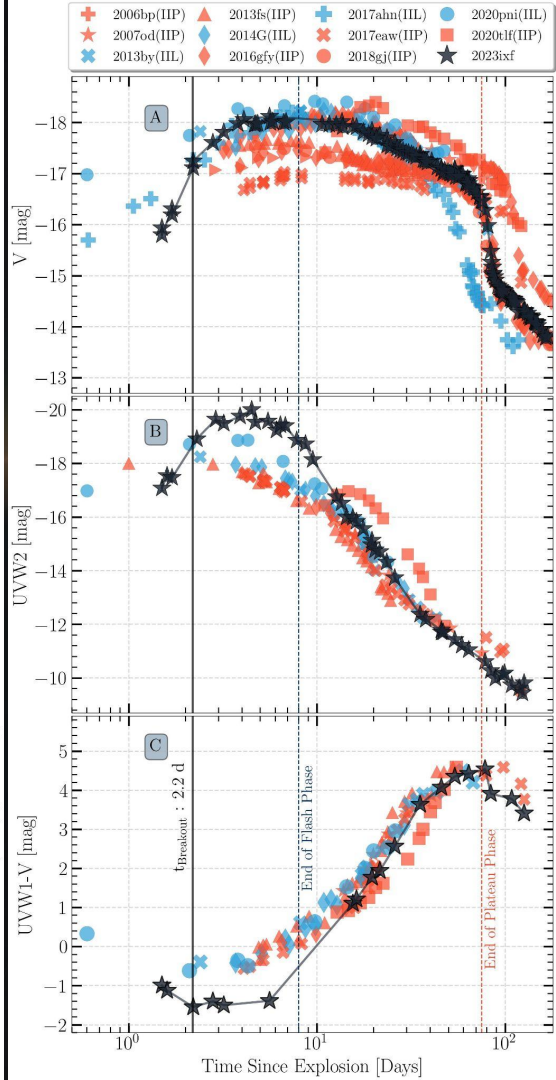


Progenitor of 2023ixf

Progenitor of 2023ixf

Kilpatrick+ 2023

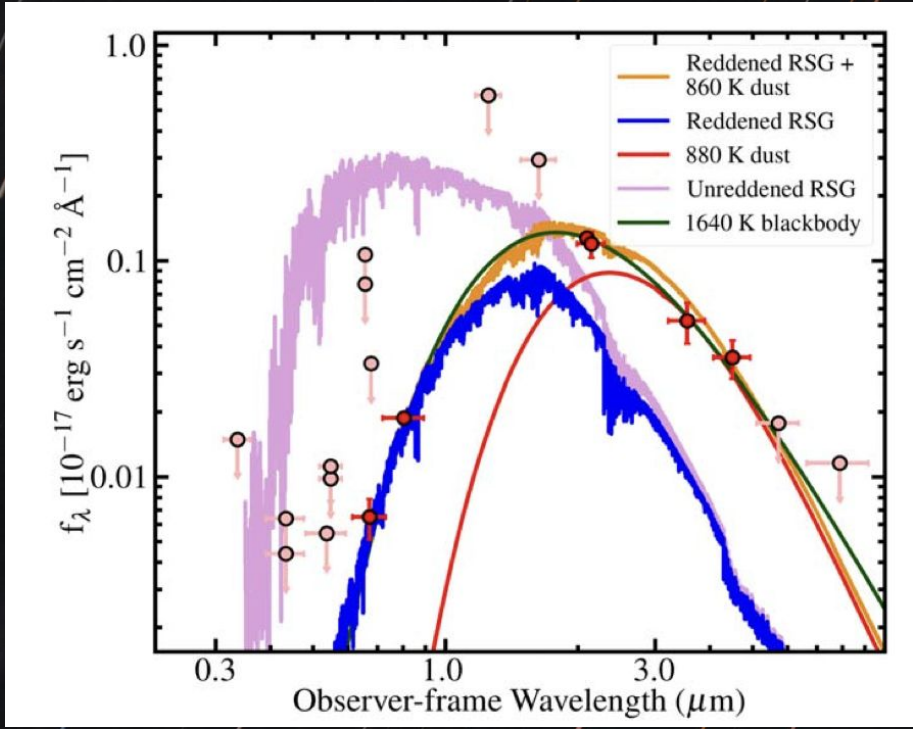

MARCS Reddened RSG + 900K Dust Shell

Jencson+ 2023

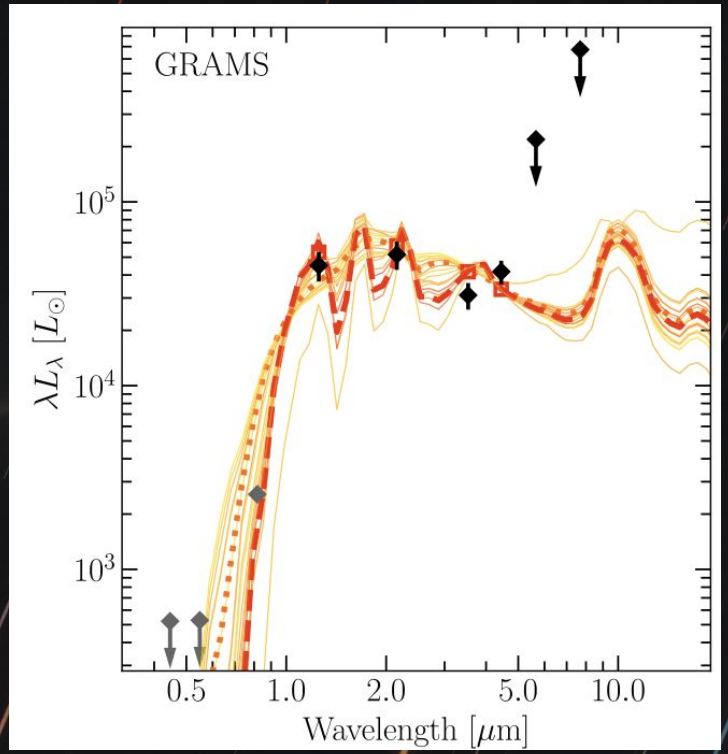

GRAMS SED Model Grid

Difference in RSG SED, Dust Prescription, **Changes ZAMS Mass**

Progenitor of 2023ixf

Kilpatrick+ 2023

Jencson+ 2023

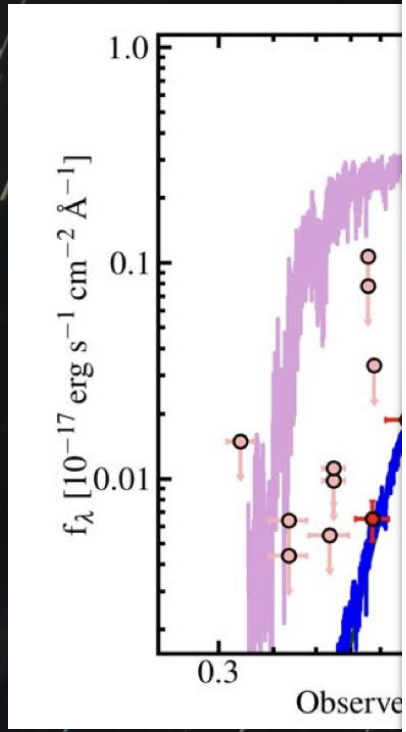

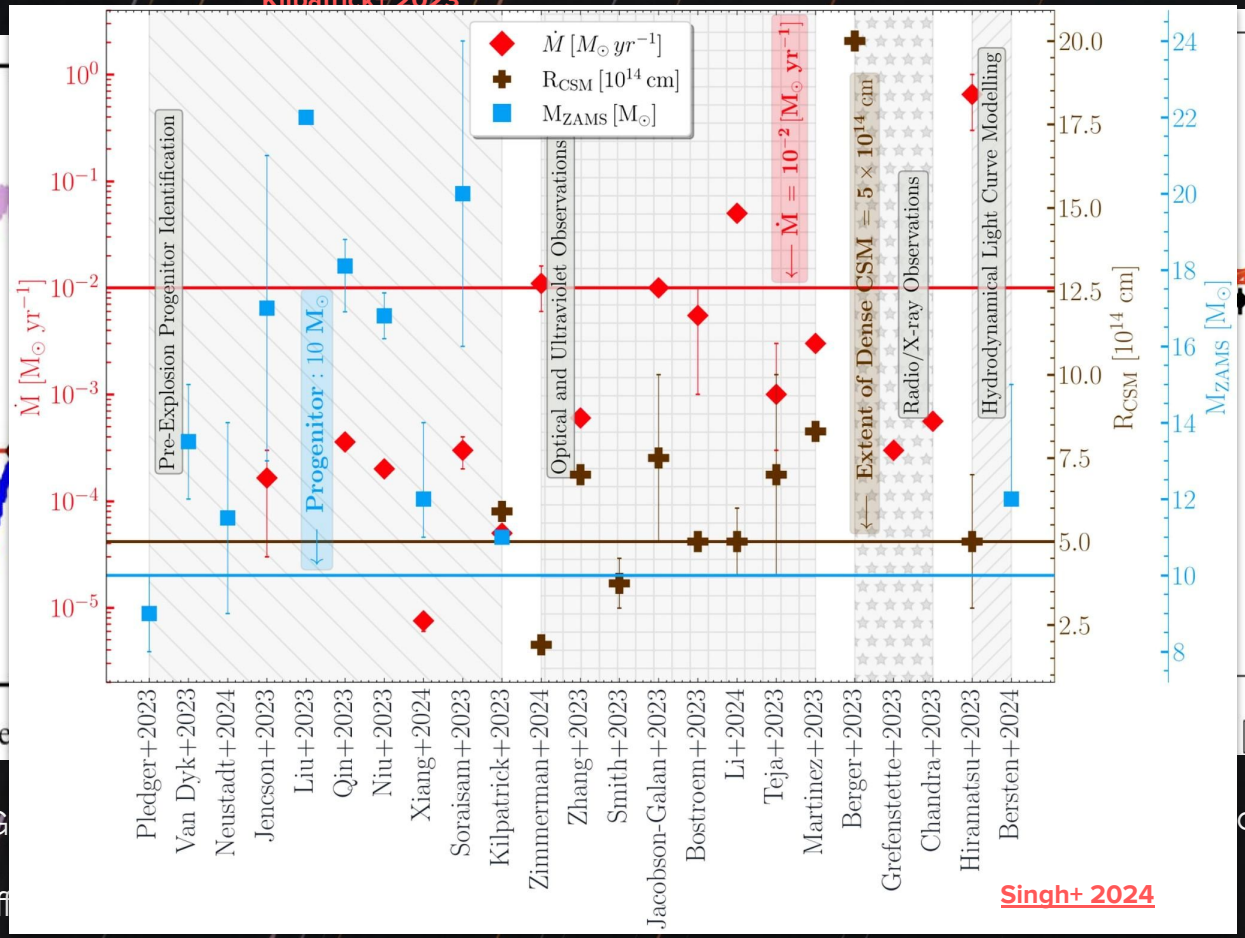

Singh+ 2024

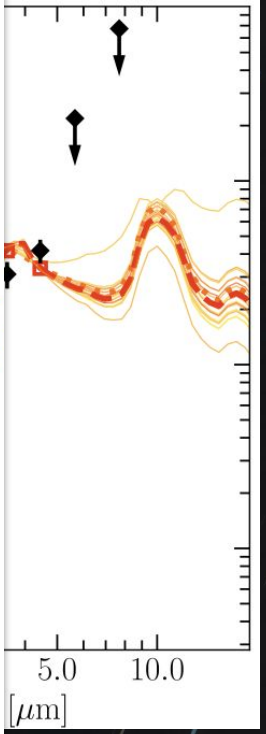

MARCS Reddened RSG

Dif

d

Progenitor of 2023ixf

Laplace+2025

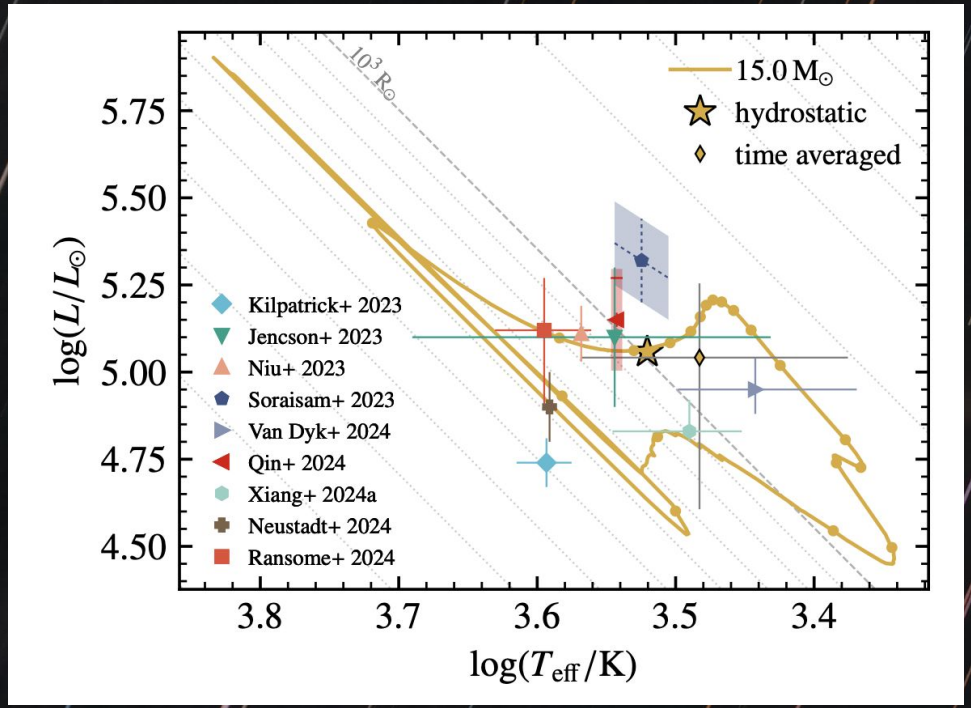

Phase folded light curve of 15 Solar mass progenitor.

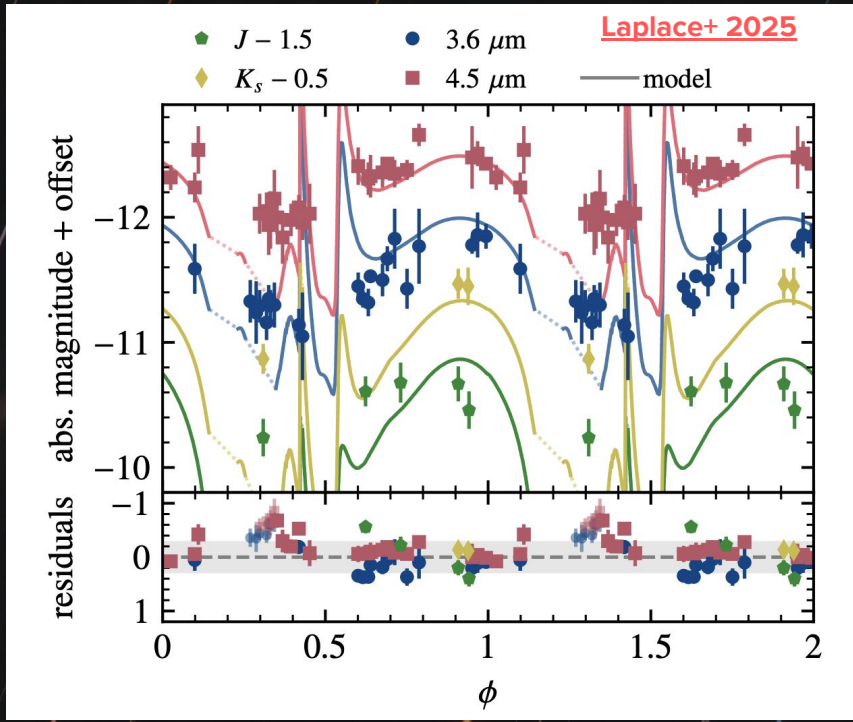

A Pulsating RSG reproduces the spread of L and Teff which can vary by up to an order of magnitudes and hence a single pre-SN HRD point cannot uniquely determine ZAMS Mass.

Pulsation naturally produces the dense dusty CSM

Signatures of Dust in 2023ixf

Optical-Infrared Light Curves

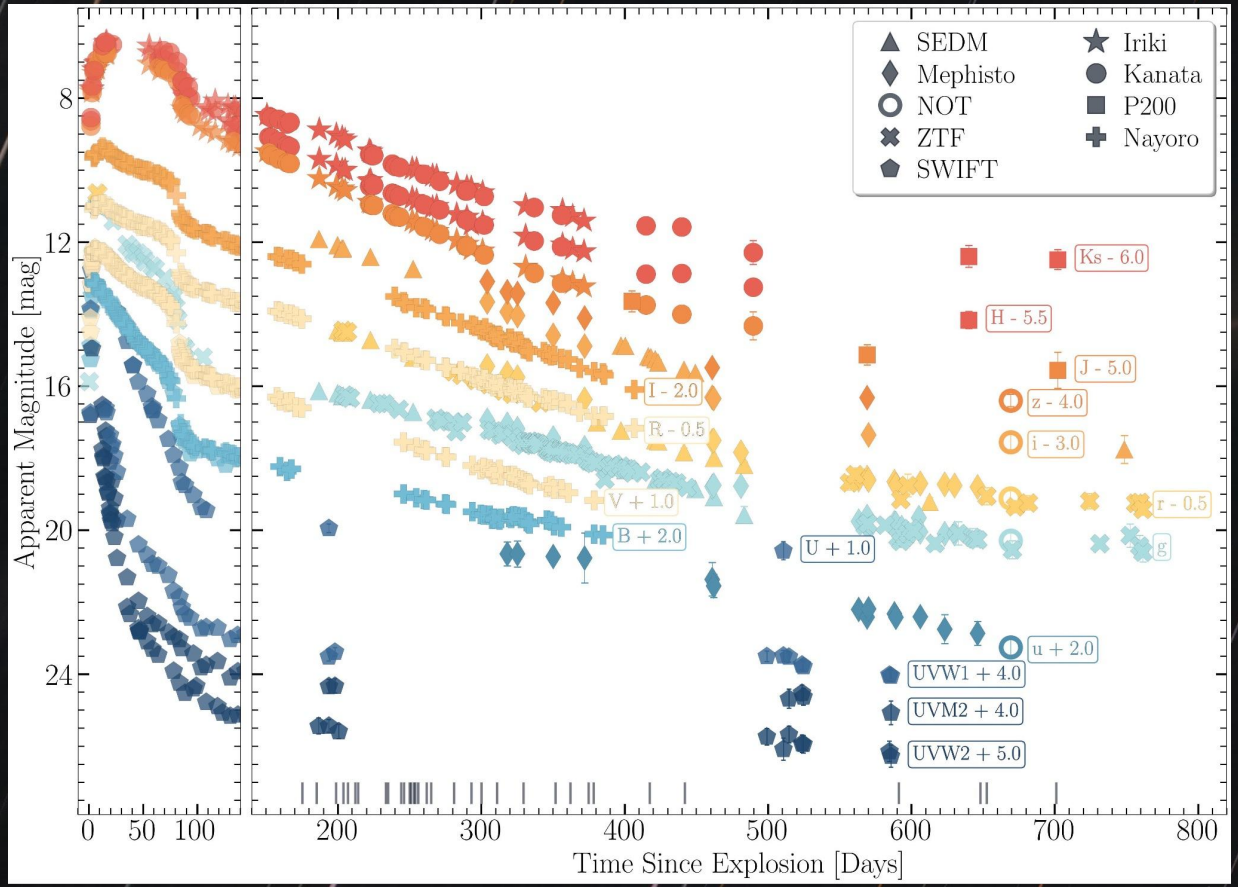

150 - 750 d Coverage

Including BVRI coverage from an Amateur Astronomer

Light C

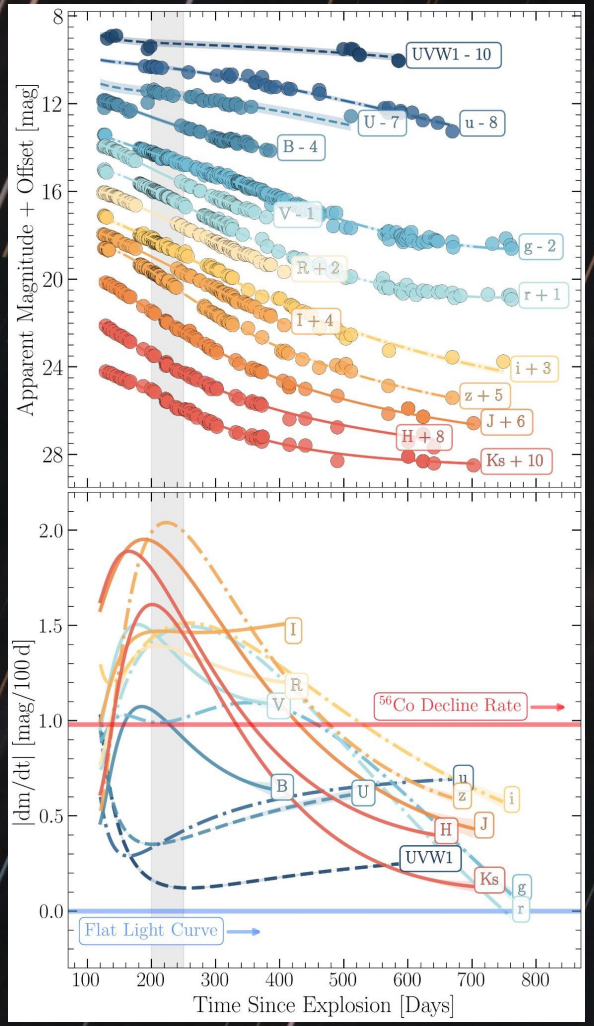

Declines steeply than 56Ni powered decay

Decline rates transition around 250d.

- Opt/IR becomes flatter
- UV steepenes

UV/Opt light curves flattening - **Shock Pow**

IR Light curves flattening - **IR excess throu**

Infrared Color Excess →

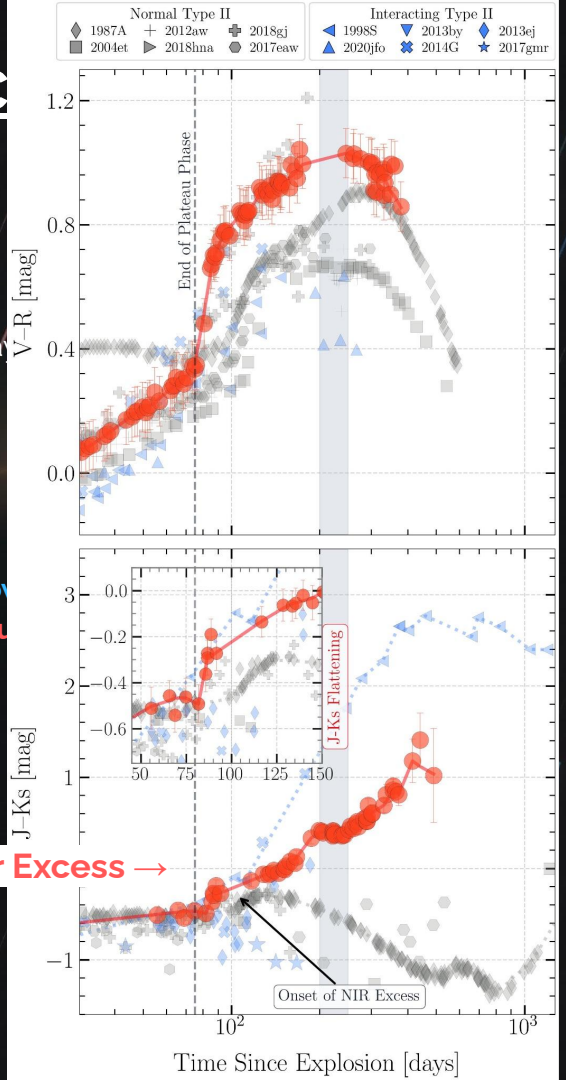

Optical Spectroscopic Sequence

Increased Redward obscuration of Halpha with time.

Shock powered CSM horns become stronger with time.

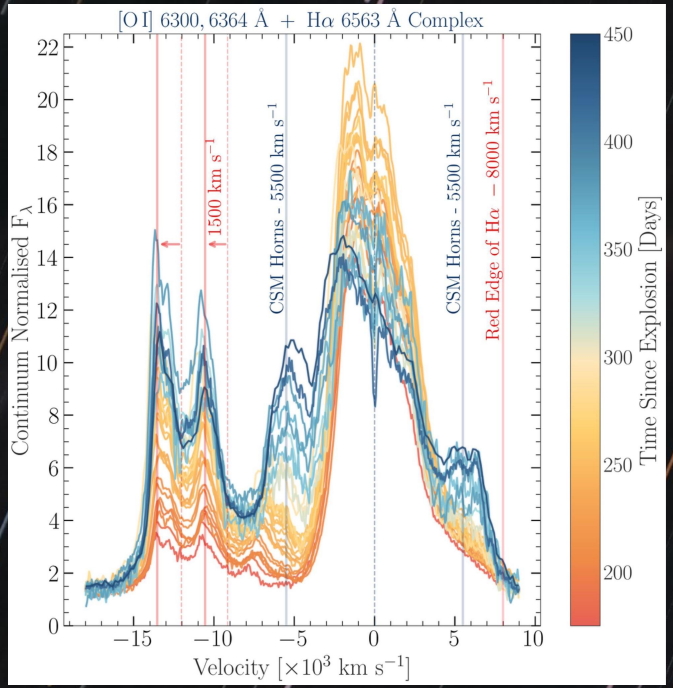

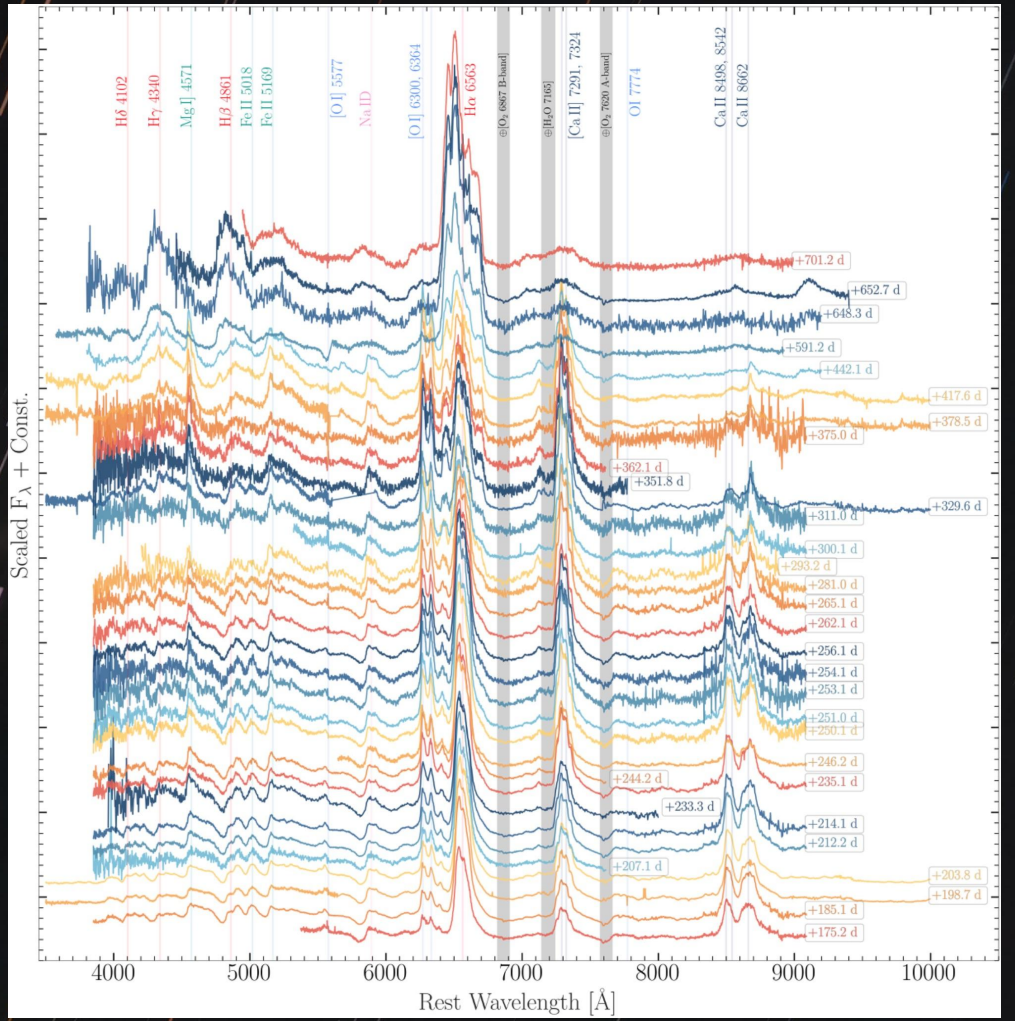

NIR Spectroscopic Sequence

- Molecular CO detection at 217d. Non detection at 8
- Asymmetry in Halpha replicated in Pa-gamma
- Presence of thermal dust clearly seen in 90 d! 217 d

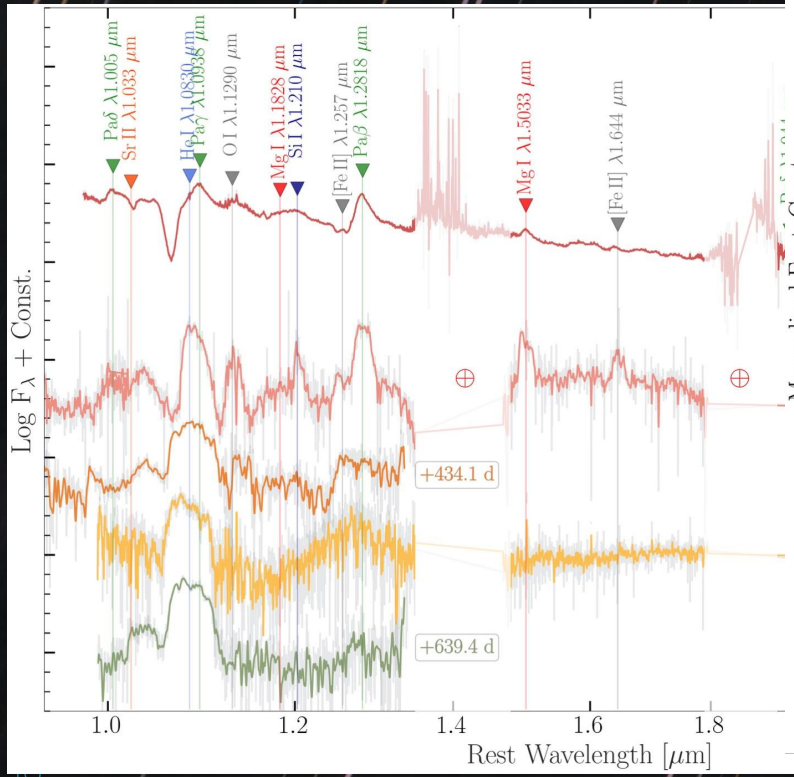

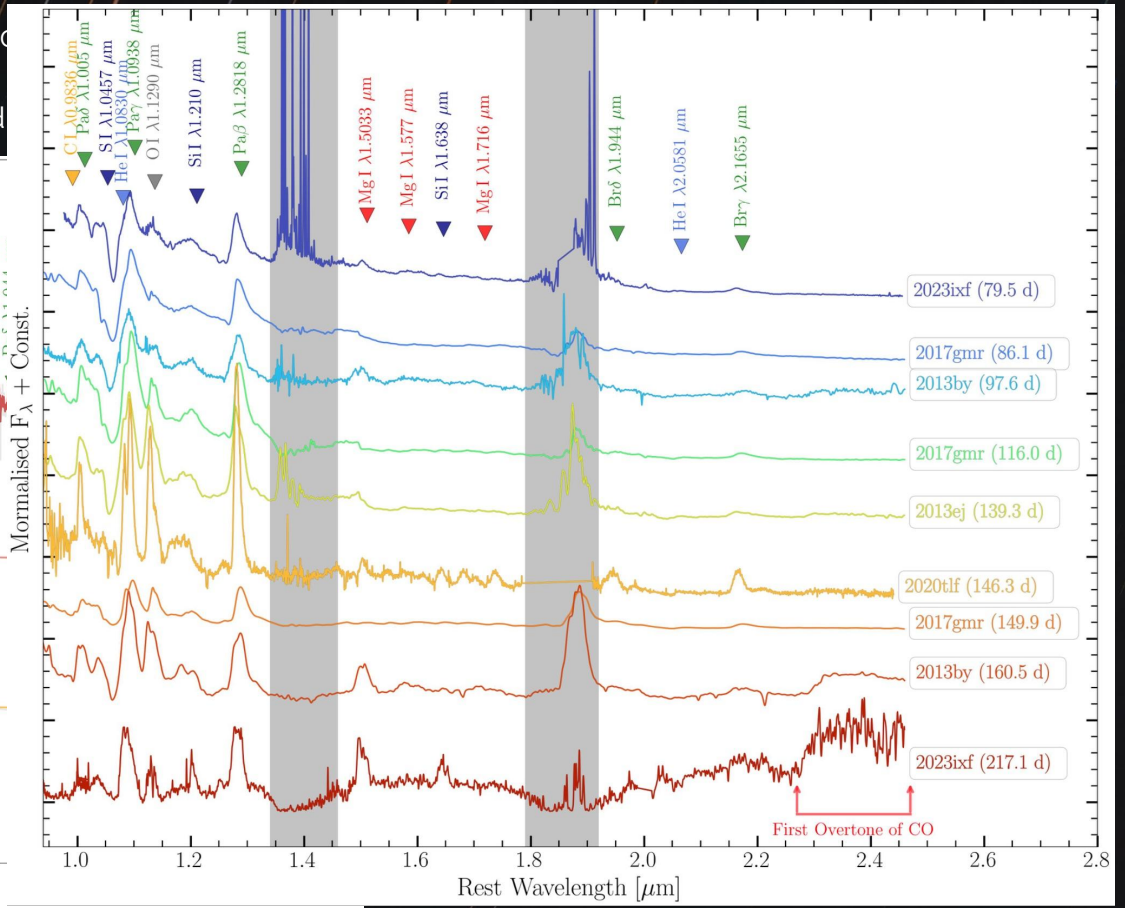

Bolometric Light Curve

Flattening is imminent in the bolometric light curve at around 500d.

Rise in % UV flux at around 400d. **(Shock-Powered Emission)**

Rise in IR/Opt flux at around 400d **(Dust)**

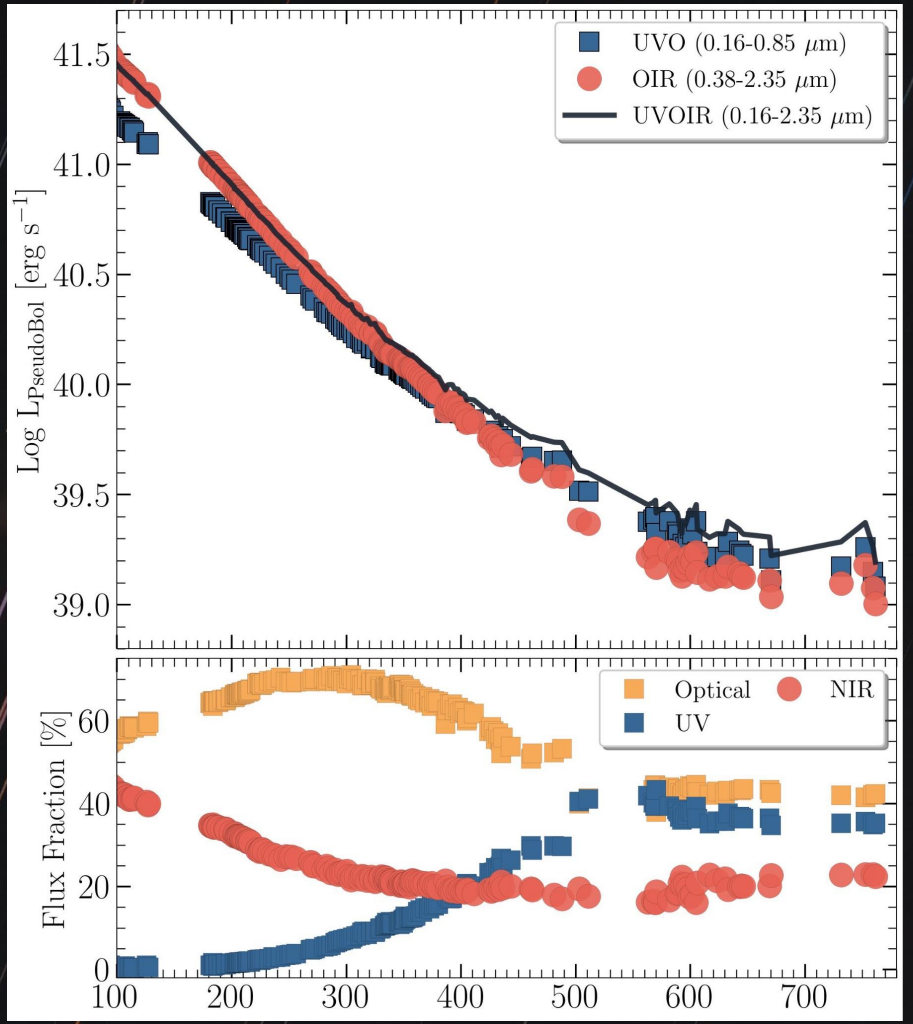

Early Rapid Dust Sublimation (< 0.3 d)

Li+ 2024

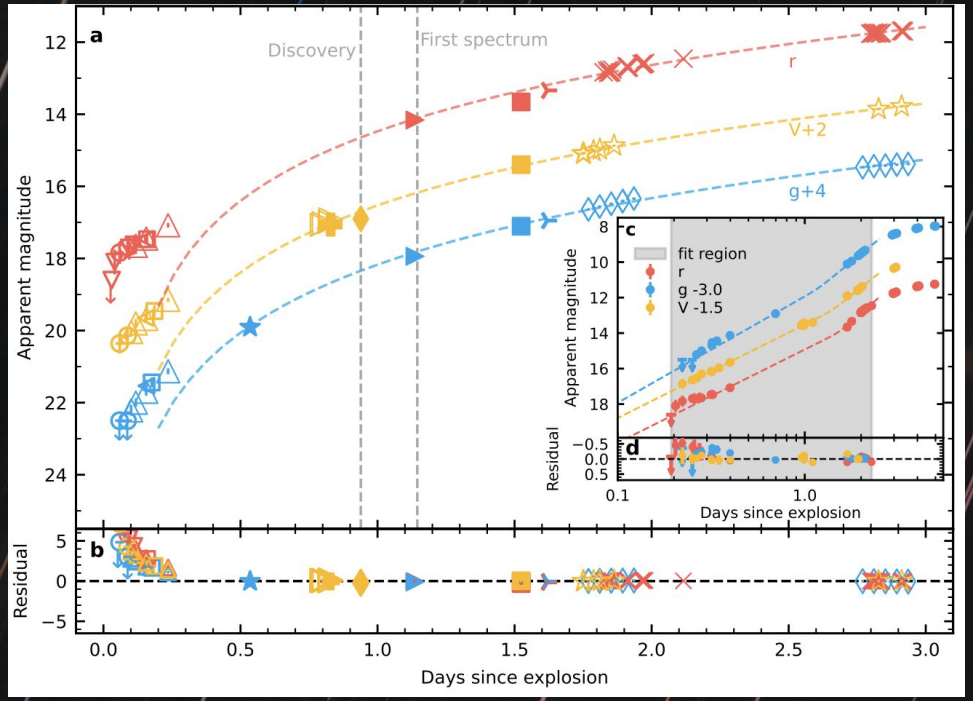

Early light curve and colours are too red to be explained by a bare shock breakout and cooling envelope.

Li+ 2024

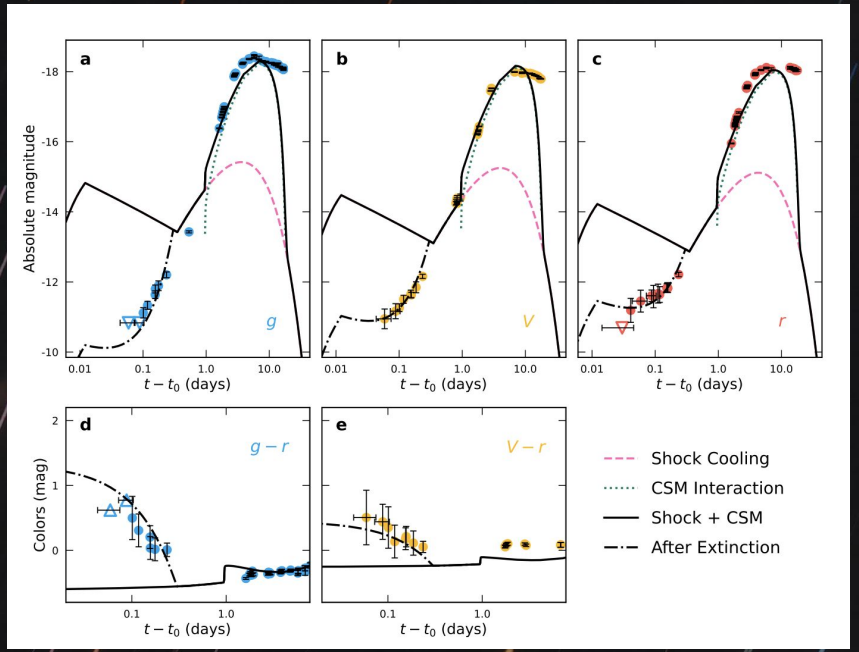

Li+24 introduce a time-varying extinction term. Line-of-sight optical depth drops as circumstellar dust grains are thermally sublimated by the intense UV/optical breakout flash.

Optically thick dust shell located very close to the star, with grains destroyed on “hour” timescales

Early IR Excess (> 1 d)

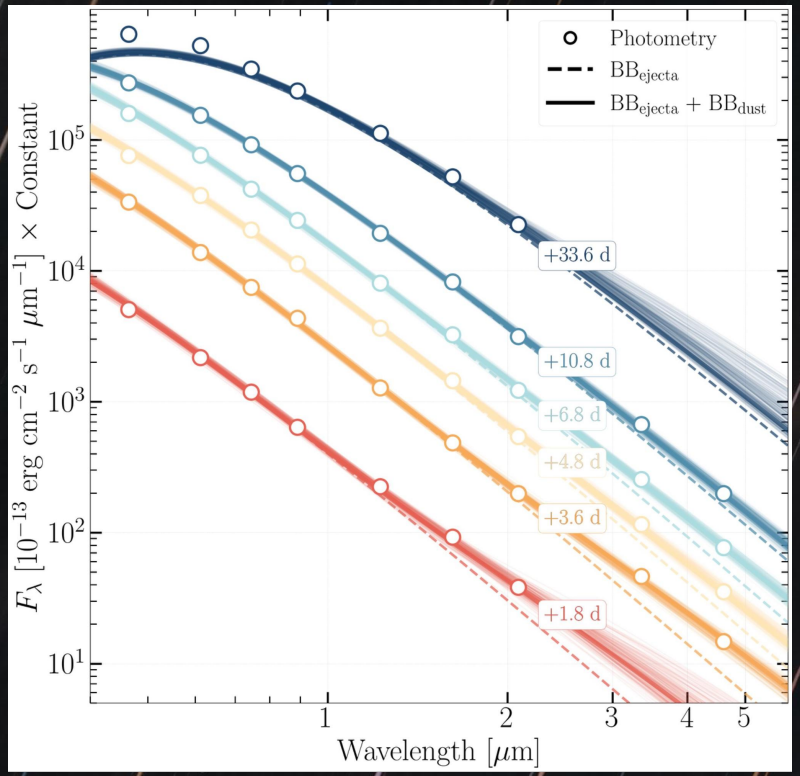

Data Source: Singh+ 2024, VanDyk+2024

A Single BB component couldn't reproduced the early phase SEDs (dashed-lines) from 1.8-10.8d.

Excess is prominent in Ks-band but is even more evident in WISE bands.

We modelled the SED with two BB components to account for the IR excess using **RedBack**.

Phase (d)	T_{hot} (K)	R_{hot} (10^{14} cm)	T_{cool} (K)	R_{cool} (10^{15} cm)
1.8	20480^{+4650}_{-3000}	$2.2^{+0.4}_{-0.4}$	2190^{+910}_{-980}	$1.1^{+2.3}_{-0.4}$
3.6	19190^{+2840}_{-2030}	$4.2^{+0.5}_{-0.5}$	1650^{+640}_{-450}	$2.2^{+1.1}_{-0.7}$
4.8	15710^{+1770}_{-1310}	$5.7^{+0.5}_{-0.6}$	1810^{+930}_{-640}	$1.7^{+1.2}_{-0.6}$
6.8	14930^{+1750}_{-1300}	$6.2^{+0.6}_{-0.7}$	2070^{+910}_{-820}	$1.6^{+1.1}_{-0.5}$
10.8	10420^{+630}_{-510}	$9.2^{+0.6}_{-0.7}$	1840^{+980}_{-690}	$1.6^{+1.3}_{-0.7}$
33.6	6030^{+50}_{-20}	$15.0^{+0.4}_{-0.5}$	1620^{+1310}_{-600}	$2.2^{+6.0}_{-1.3}$

Early IR Exc

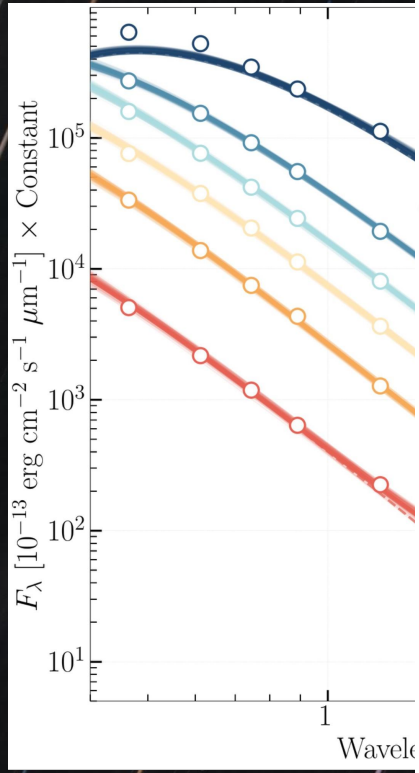

Data Source: Sin

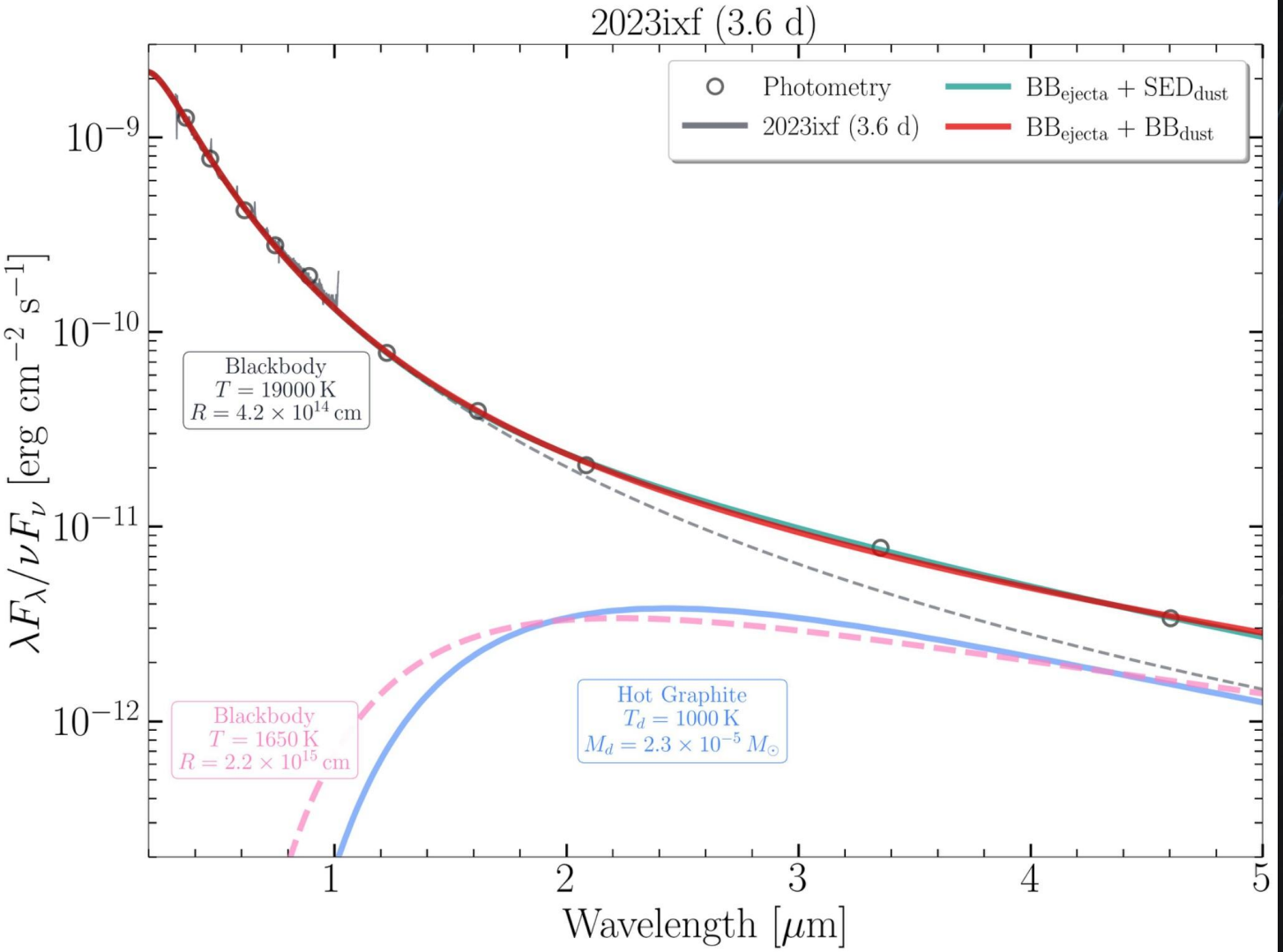

Early IR Exc

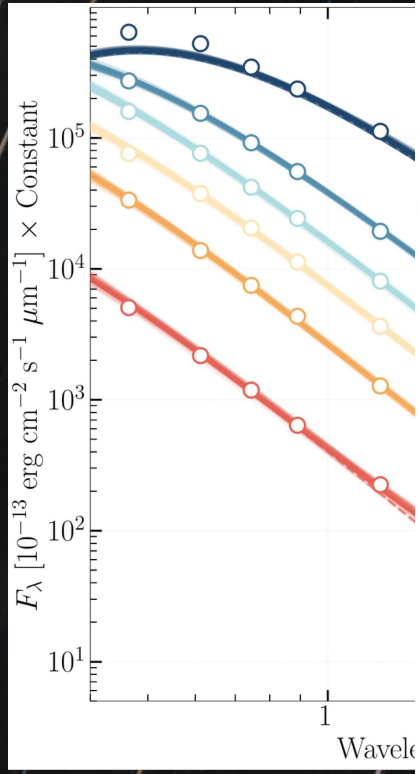

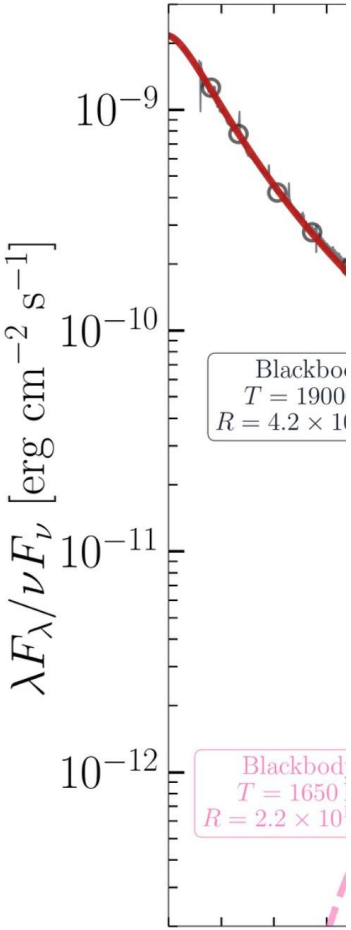

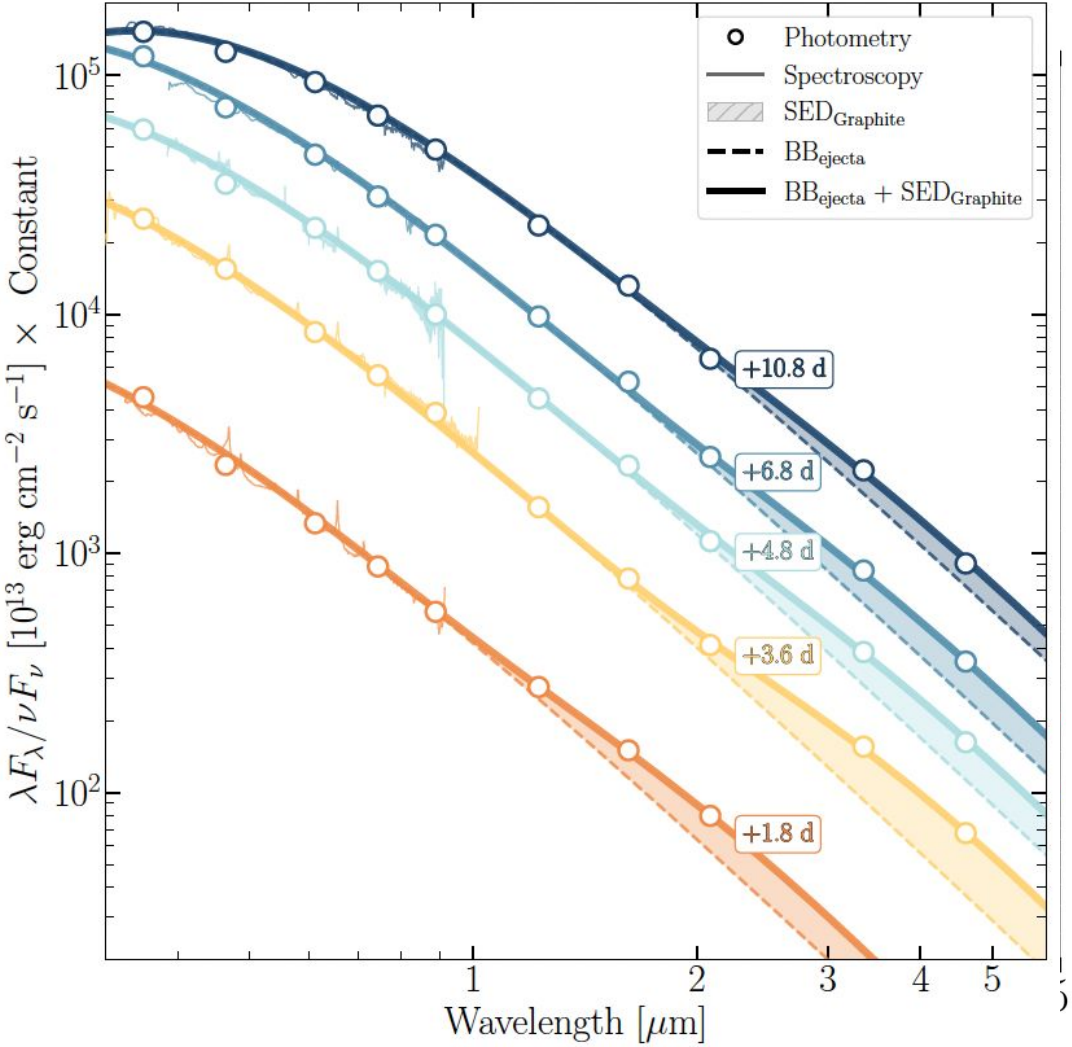

Data Source: Sin

Early IR Exc

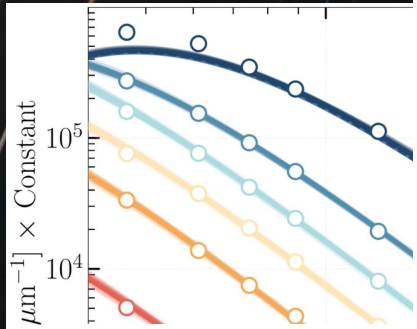

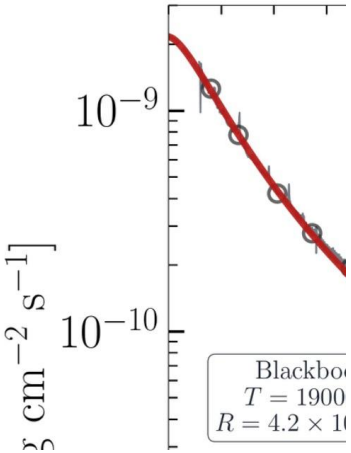

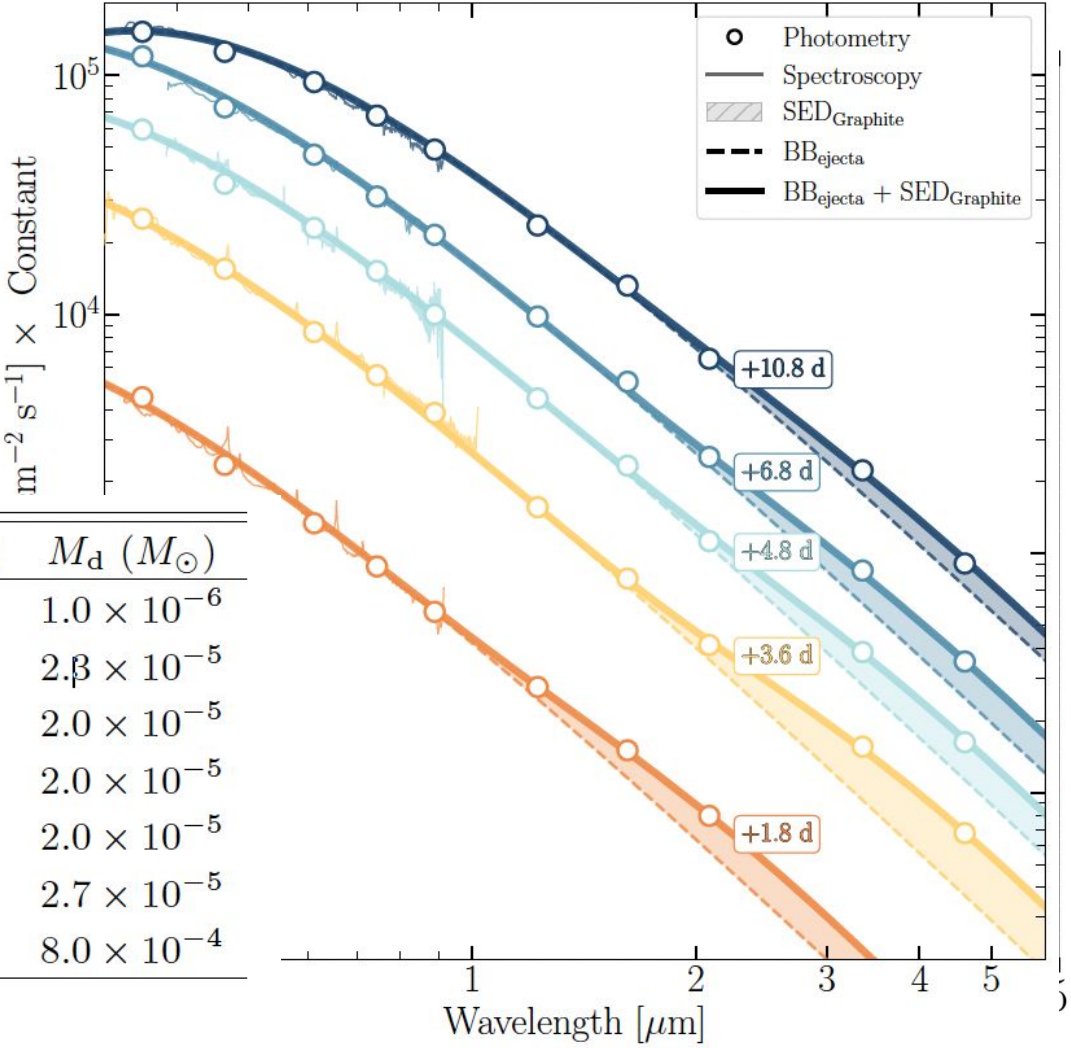

Epoch (d)	Dust	$T_{\rm d}$ (K)	$M_{\rm d}$ ($M_\odot$)
1.8	Graphite (Hot)	1650	1.0×10^{-6}
3.6	Graphite (Hot)	1000	2.3×10^{-5}
4.8	Graphite (Hot)	1000	2.0×10^{-5}
6.8	Graphite (Hot)	1000	2.0×10^{-5}
10.8	Graphite (Hot)	1000	2.0×10^{-5}
33.6	Graphite (Hot)	1000	2.7×10^{-5}
33.6	Graphite (Cold)	440	8.0×10^{-4}

Photospheric MIR Excess (33.6 d)

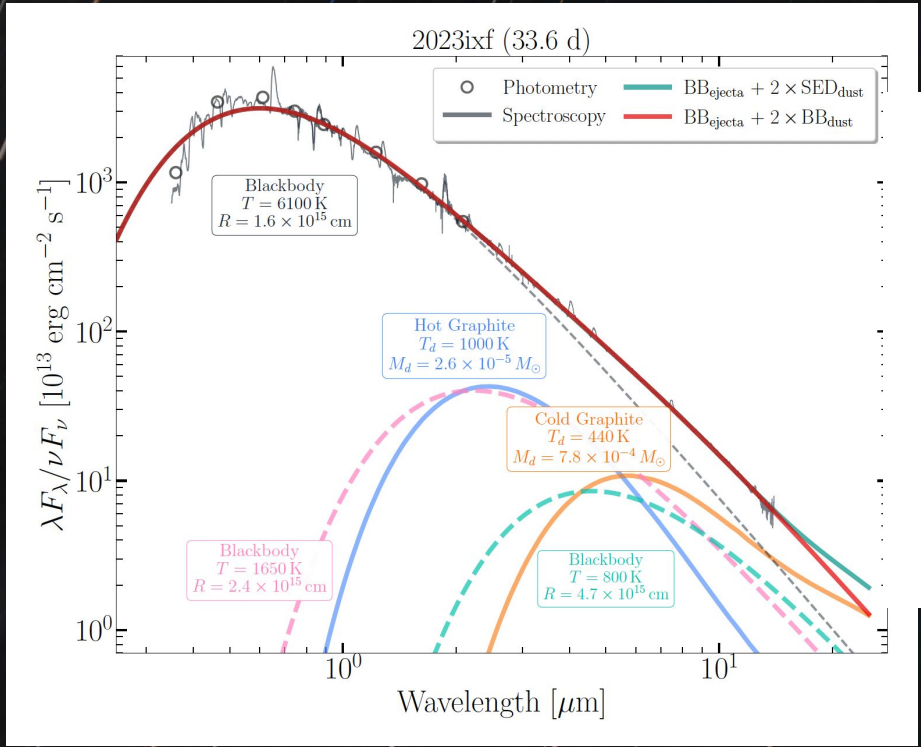

Epoch (d)	Dust	T_d (K)	M_d ($M_\odot$)
1.8	Graphite (Hot)	1650	1.0×10^{-6}
3.6	Graphite (Hot)	1000	2.3×10^{-5}
4.8	Graphite (Hot)	1000	2.0×10^{-5}
6.8	Graphite (Hot)	1000	2.0×10^{-5}
10.8	Graphite (Hot)	1000	2.0×10^{-5}
33.6	Graphite (Hot)	1000	2.7×10^{-5}
33.6	Graphite (Cold)	440	8.0×10^{-4}

Data Source: Derkacy+25

RSG stars are supposed to have Oxygen-rich winds (rich in Silicates)

However, the Photospheric phase IR echo does not show any Silicate Bump

Nebular Phase IR Excess (> 90 d)

- In the departure from photospheric phase, we start seeing excess in Ks band beginning 89 d in our SED.
- The excess becomes prominent in H-band beginning 213 d.
- We modelled the SED with two BB components to account for the IR excess using **RedBack**.

Phase (d)	T_{BB} (K)	R_{BB} (10^{14} cm)	T_{Dust} (K)	R_{Dust} (10^{15} cm)
89.0	4330^{+80}_{-80}	$12.0^{+0.6}_{-0.6}$	590^{+260}_{-70}	$41.0^{+97.0}_{-35.0}$
129.0	4560^{+100}_{-90}	$8.3^{+0.5}_{-0.5}$	600^{+280}_{-80}	$47.0^{+91.0}_{-40.0}$
175.0	4940^{+130}_{-120}	$5.1^{+0.3}_{-0.3}$	590^{+220}_{-70}	$76.0^{+99.0}_{-60.0}$
213.0	5270^{+150}_{-140}	$3.4^{+0.2}_{-0.2}$	810^{+70}_{-70}	$12.0^{+3.3}_{-2.4}$
252.0	5740^{+190}_{-170}	$2.2^{+0.2}_{-0.1}$	810^{+60}_{-60}	$10.0^{+2.1}_{-1.7}$
271.0	6060^{+210}_{-200}	$1.8^{+0.1}_{-0.1}$	800^{+50}_{-50}	$10.0^{+1.7}_{-1.4}$
302.0	6560^{+250}_{-230}	$1.3^{+0.1}_{-0.1}$	810^{+40}_{-40}	$8.9^{+1.3}_{-1.0}$
331.0	6820^{+310}_{-260}	$1.0^{+0.1}_{-0.1}$	820^{+40}_{-40}	$7.7^{+1.0}_{-0.9}$
372.0	7480^{+400}_{-360}	$0.7^{+0.1}_{-0.1}$	830^{+30}_{-30}	$6.6^{+0.8}_{-0.7}$
415.0	7990^{+670}_{-570}	$0.5^{+0.1}_{-0.1}$	900^{+130}_{-130}	$4.6^{+4.5}_{-1.9}$
553.0	8110^{+740}_{-590}	$0.5^{+0.1}_{-0.1}$	920^{+140}_{-140}	$4.2^{+3.9}_{-1.7}$
600.0	8670^{+1270}_{-1000}	$0.2^{+0.0}_{-0.0}$	1000^{+120}_{-100}	$2.4^{+1.3}_{-0.8}$
623.0	9370^{+1480}_{-1090}	$0.2^{+0.0}_{-0.0}$	1020^{+110}_{-90}	$2.0^{+0.9}_{-0.6}$
649.0	11940^{+1770}_{-1630}	$0.1^{+0.0}_{-0.0}$	1170^{+80}_{-80}	$1.4^{+0.4}_{-0.3}$

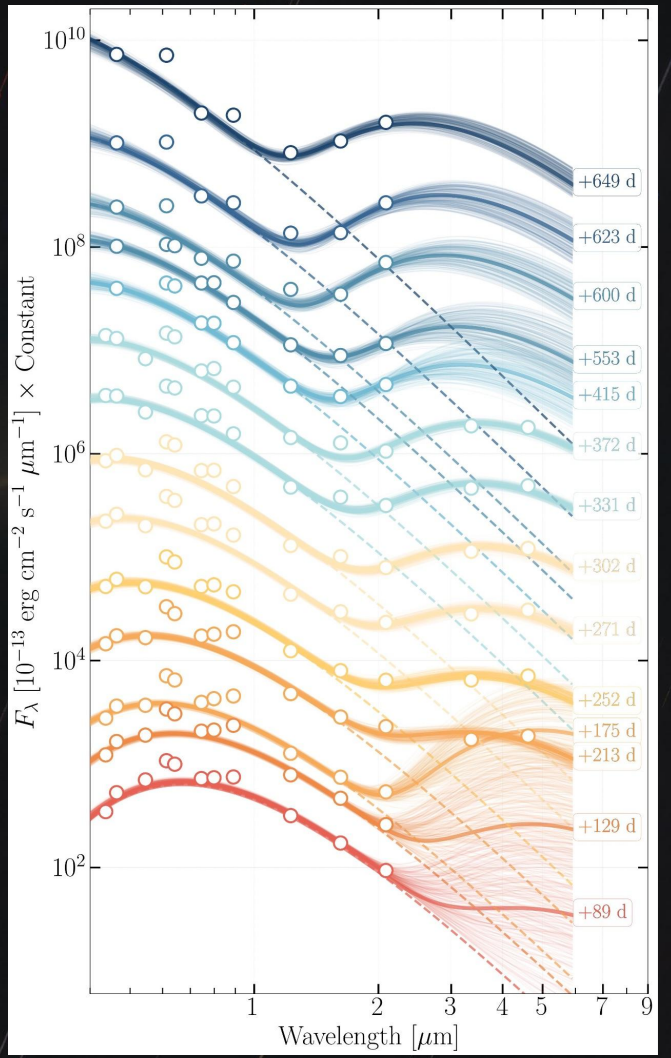

Late Nebular Phase - SED Fitting

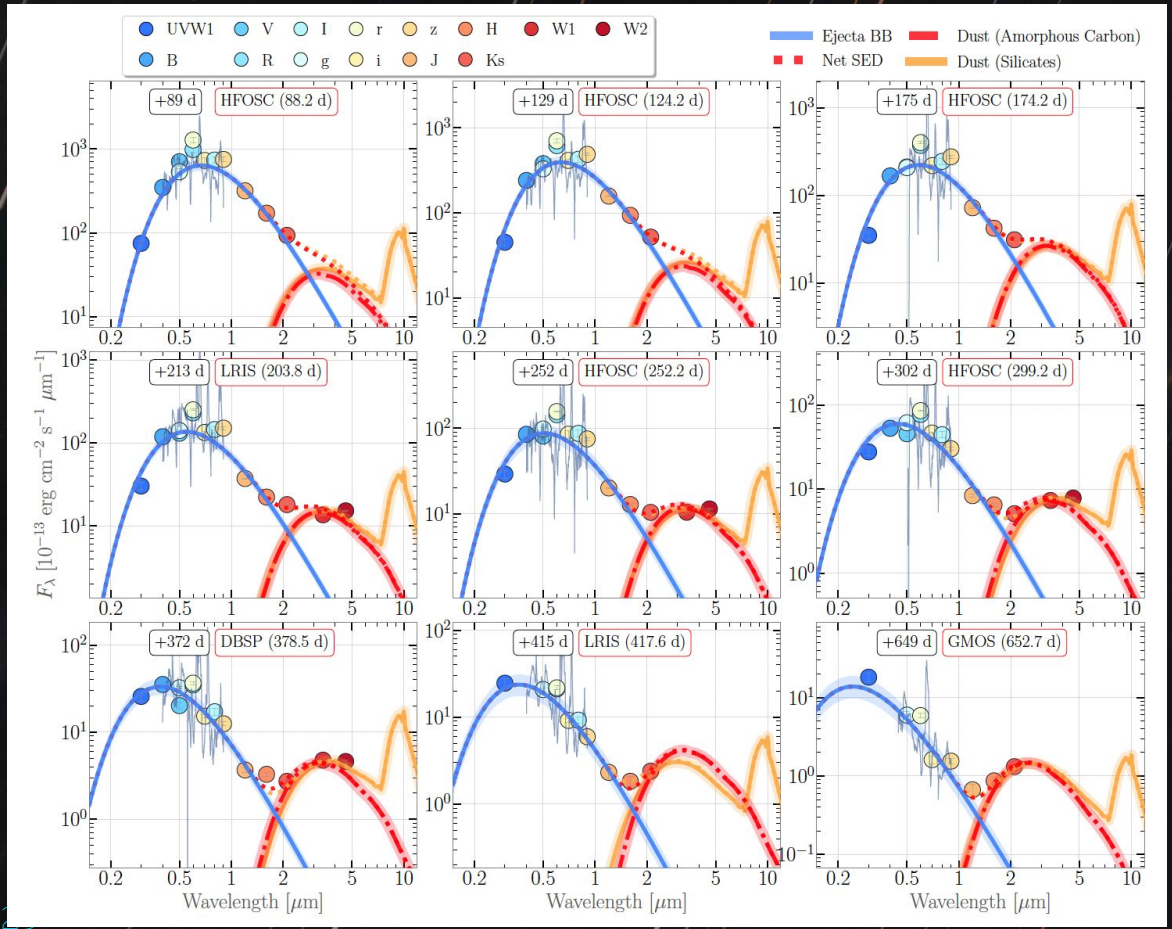

- We model the SED with two components: a hot photospheric blackbody and a cooler dust component.
- The hot blackbody serves as a smooth ejecta continuum (ignoring strong line regions and non-LTE effects).

- The dust emission is calculated for optically thin Mie grains (amorphous carbon and astronomical silicate) with a fixed small grain radius of 0.1 microns,
- Dust prescription from Kato+2009, Gall+2014.

- Dust mass could be rescaled to other grain sizes using (remains nearly unchanged within the Rayleigh regime, 0.01–0.1 micron)

Late Nebular Phase - SED Fitting

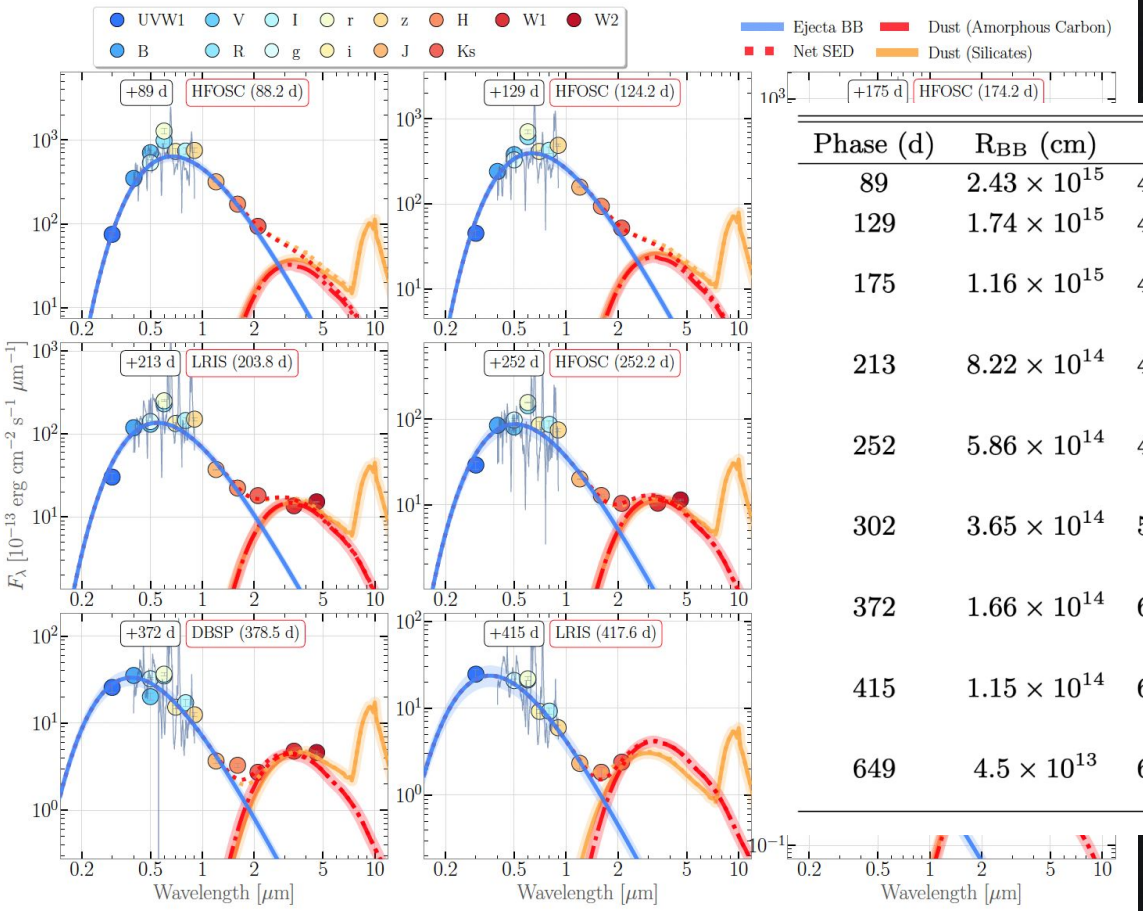

Phase (d)	R_{BB} (cm)	T_{BB} (K)	Dust Type	T_{Dust} (K)	M_{Dust} ($M_\odot$)
89	2.43×10^{15}	4120 ± 140	-	-	-
129	1.74×10^{15}	4210 ± 160	-	-	-
175	1.16×10^{15}	4400 ± 190	Graphites	400	9.0×10^{-3}
			Silicates	450	1.0×10^{-2}
213	8.22×10^{14}	4600 ± 190	Graphites	500	4.0×10^{-4}
			Silicates	550	2.0×10^{-3}
252	5.86×10^{14}	4820 ± 200	Graphites	500	3.0×10^{-4}
			Silicates	600	1.0×10^{-3}
302	3.65×10^{14}	5210 ± 230	Graphites	550	1.0×10^{-4}
			Silicates	600	7.0×10^{-4}
372	1.66×10^{14}	6260 ± 400	Graphites	600	4.0×10^{-5}
			Silicates	700	2.0×10^{-4}
415	1.15×10^{14}	6690 ± 290	Graphites	700	1.0×10^{-5}
			Silicates	700	2.0×10^{-4}
649	4.5×10^{13}	6860 ± 820	Graphites	550	8.0×10^{-5}
			Silicates	500	5.0×10^{-3}

Nebular Phase IR Excess in Optical-MIR SED(> 250 d)

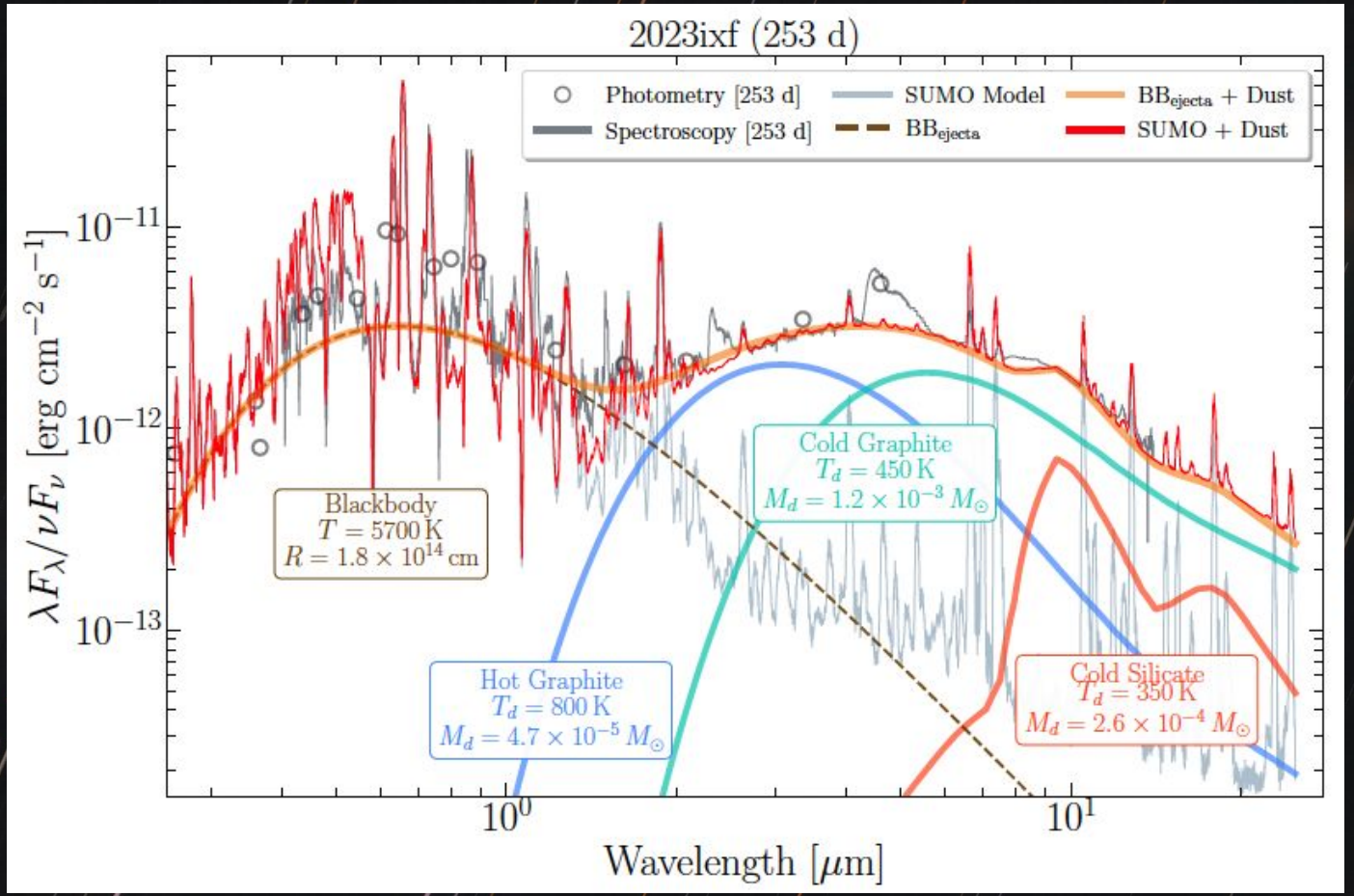

Nebular Phase IR Excess in Optical-MIR SED(> 250 d)

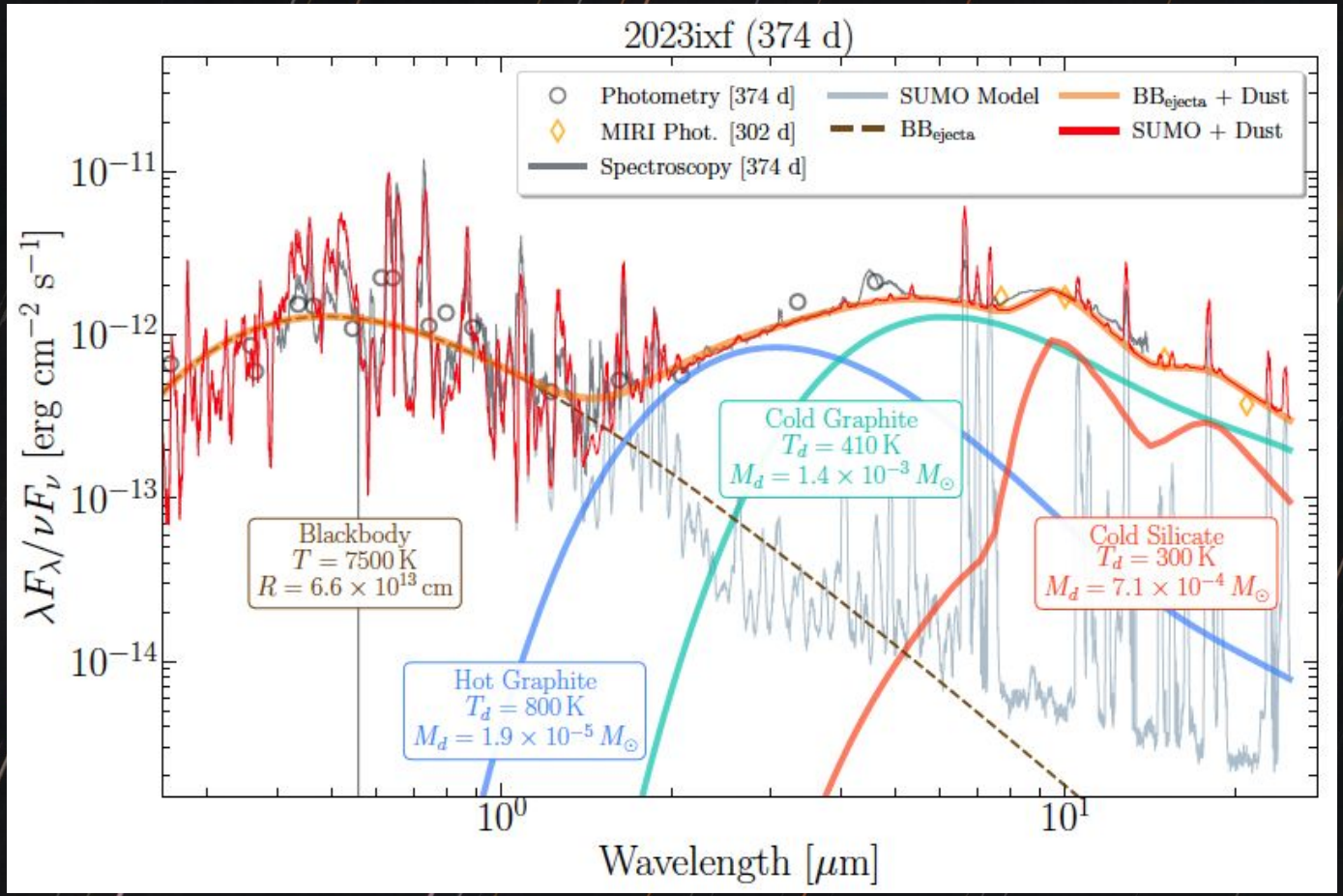

Nebular Phase IR Excess in Optical-MIR SED(> 250 d)

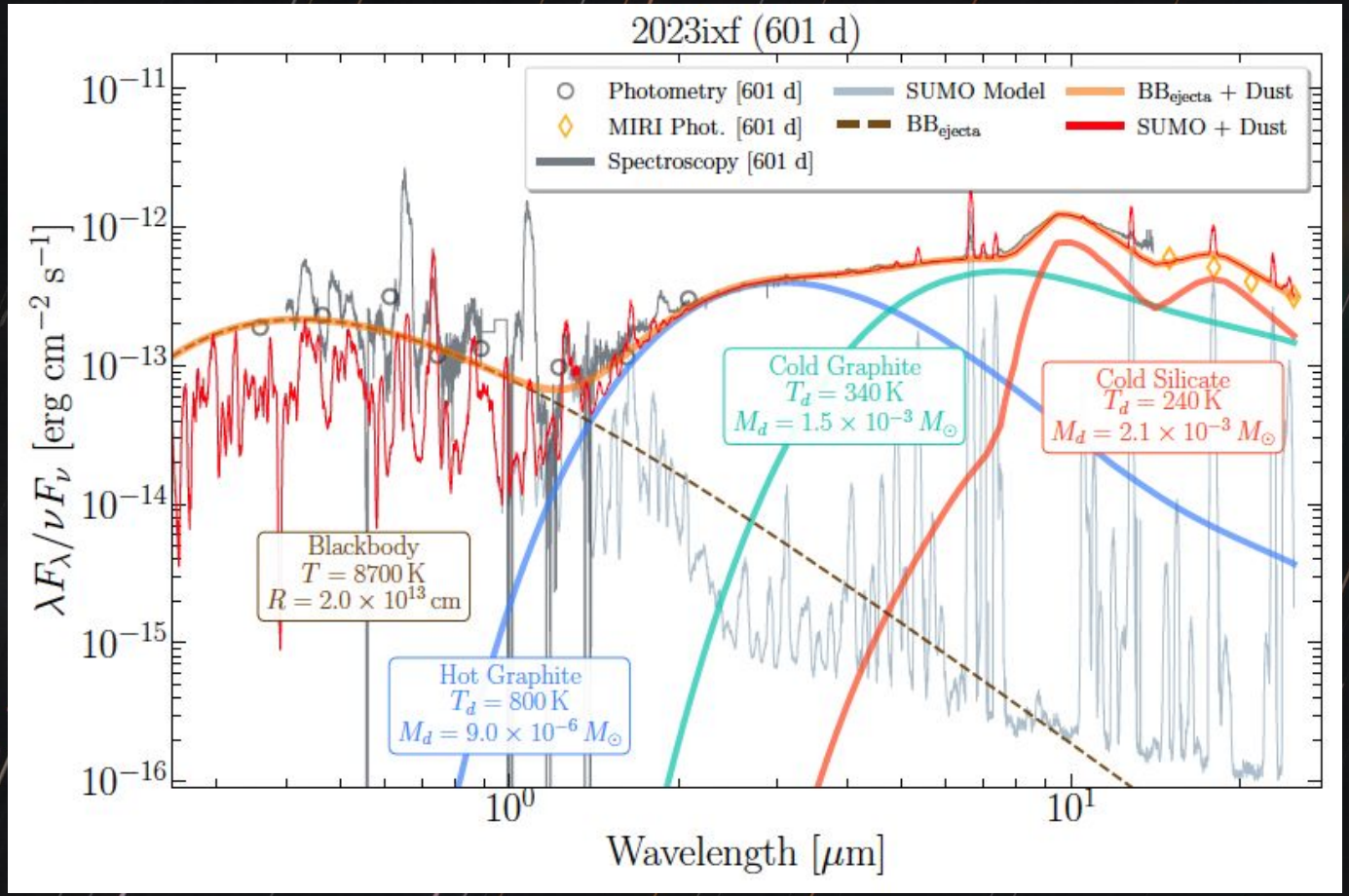

Nebular Phase IR Excess in Optical-MIR SED(> 250 d)

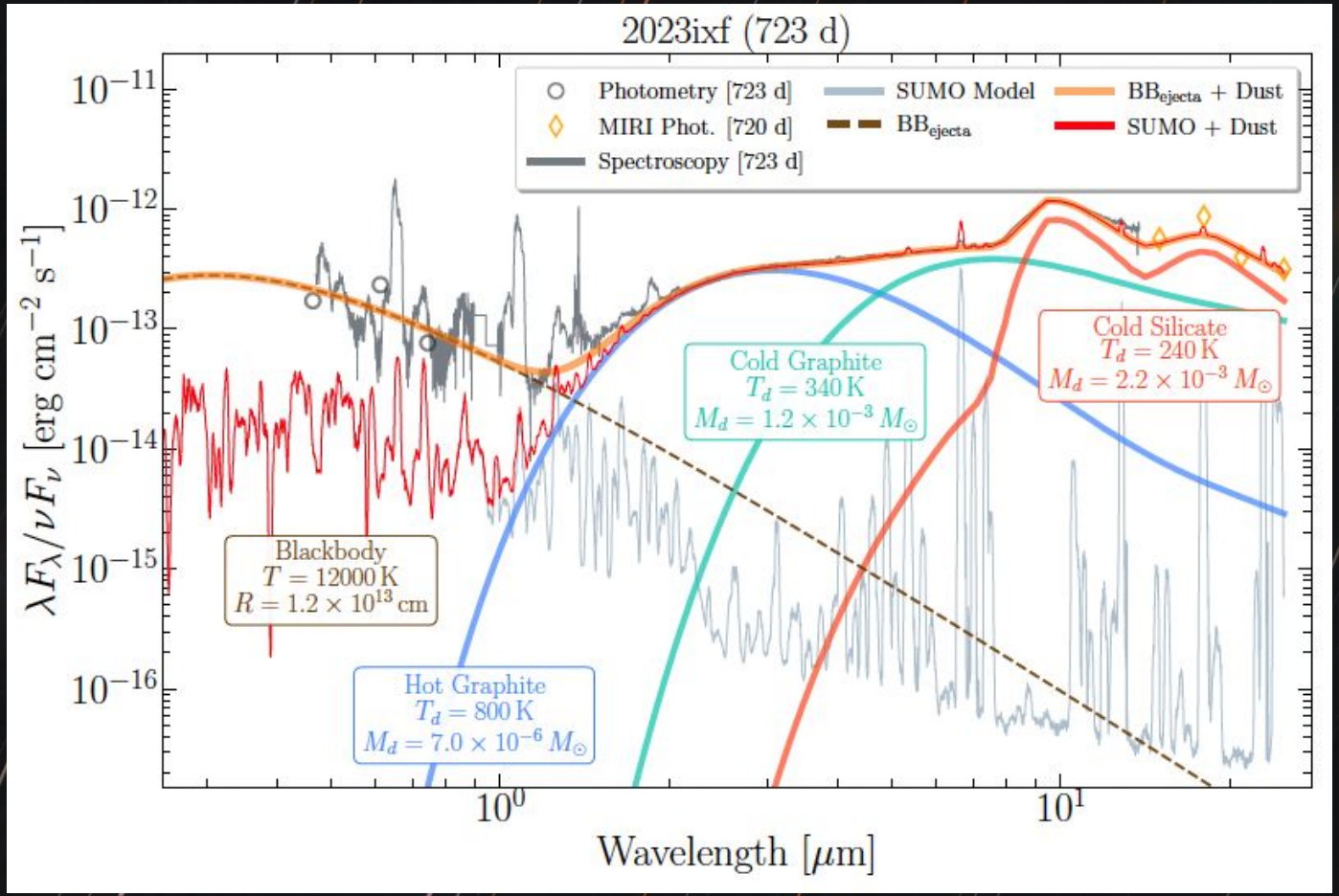

Polarisation : Asphericity Everywhere

- We see 3 peaks in the polarisation light curve.
- Peak A (1%): interaction with the **asymmetric compact dense CSM**
- Peak B (at 0.7%) : due to the H-envelope and/or the interaction with the low-density extended CSM
- Peak C (0.4%): He-core revealing itself at the end of plateau phase

Polarisation in CCSNe arises from electron scattering, which preferentially polarises the light tangentially to the photosphere (or point of last scattering).

Singh+24

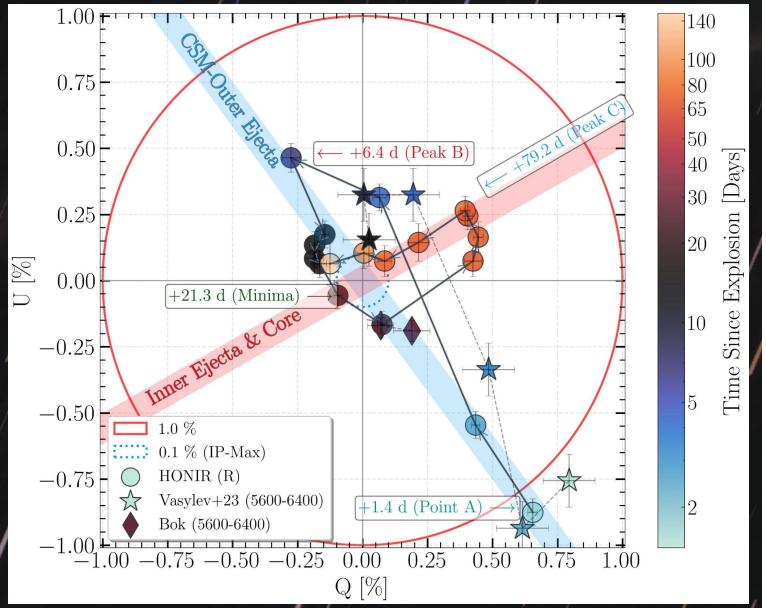

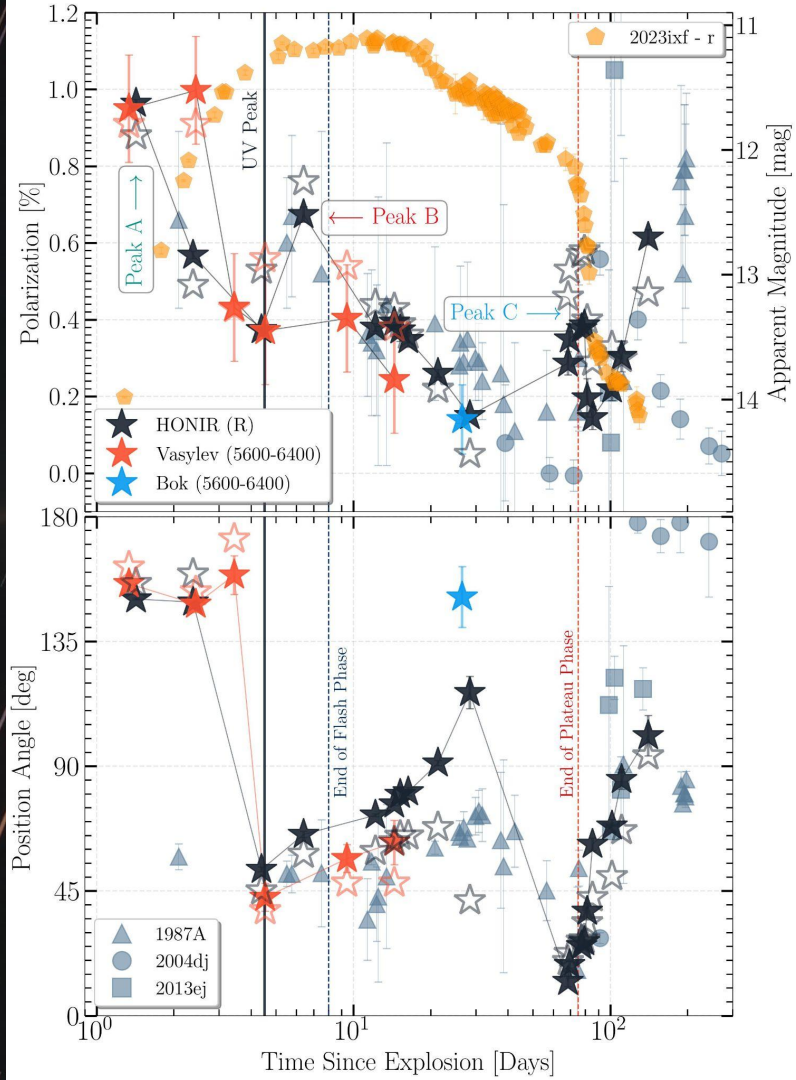

Polarisation : Asphericity Everywhere

- We see 3 peaks in the polarisation light curve.
- Peak A (1%): interaction with the **asymmetric compact dense CSM**
- Peak B (at 0.7%) : due to the H-envelope and/or the interaction with the low-density
- Peak C (0.4

Polarisation in CCS
arises from electro
scattering, which
preferentially polar
light tangentially to
photosphere (or po
last scattering).

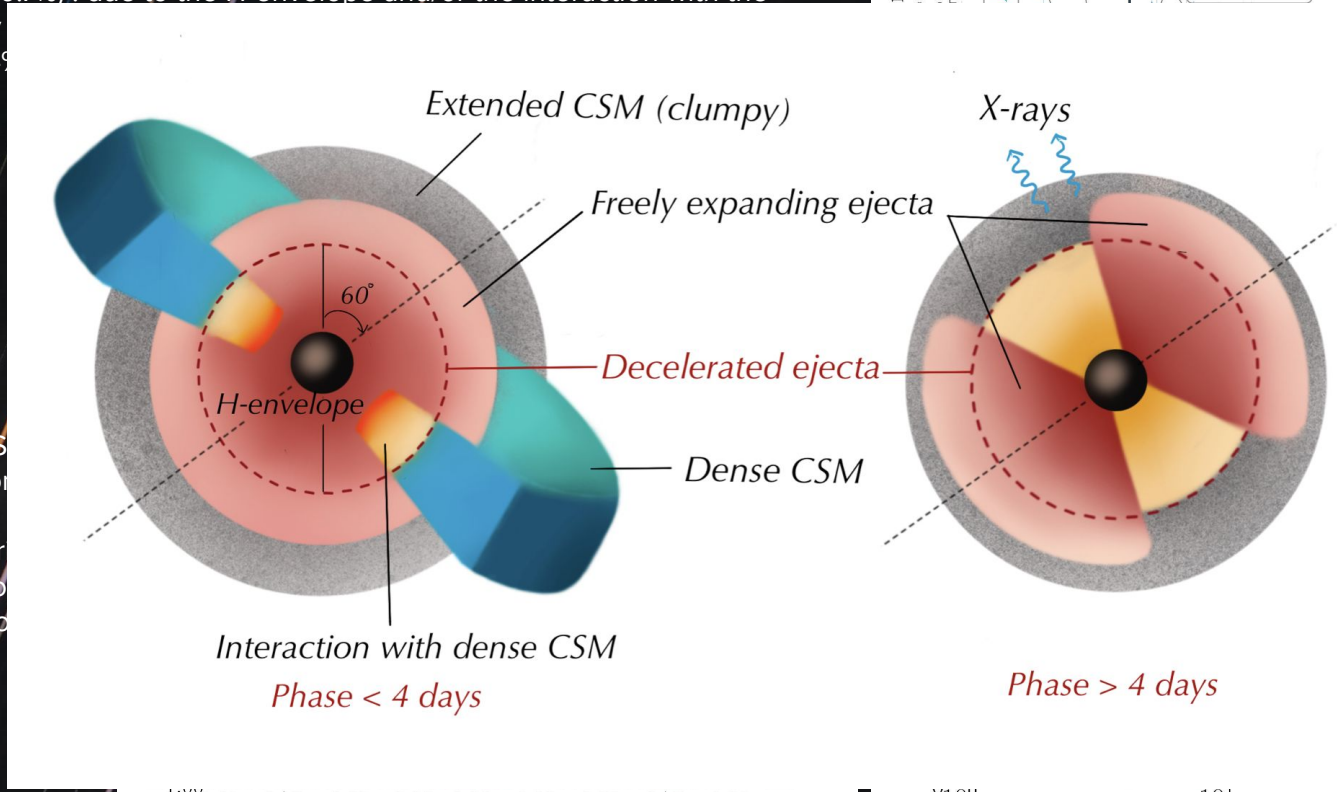

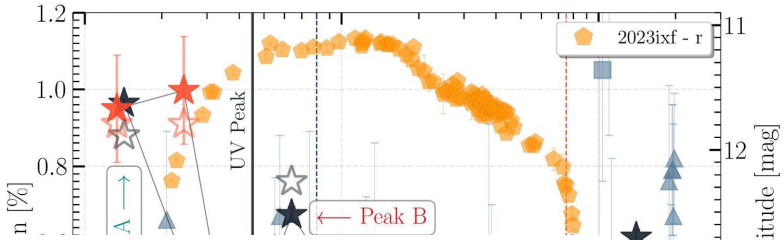

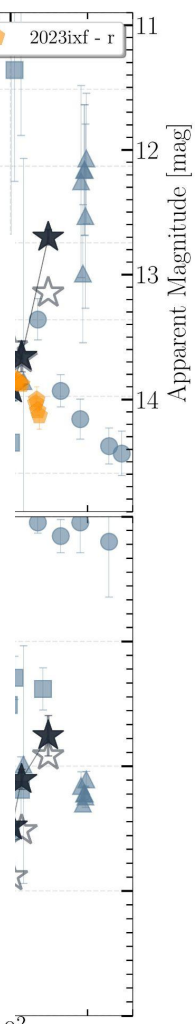

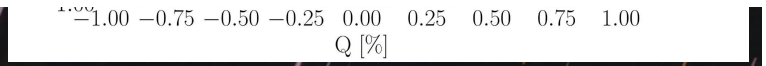

Early IR Echo

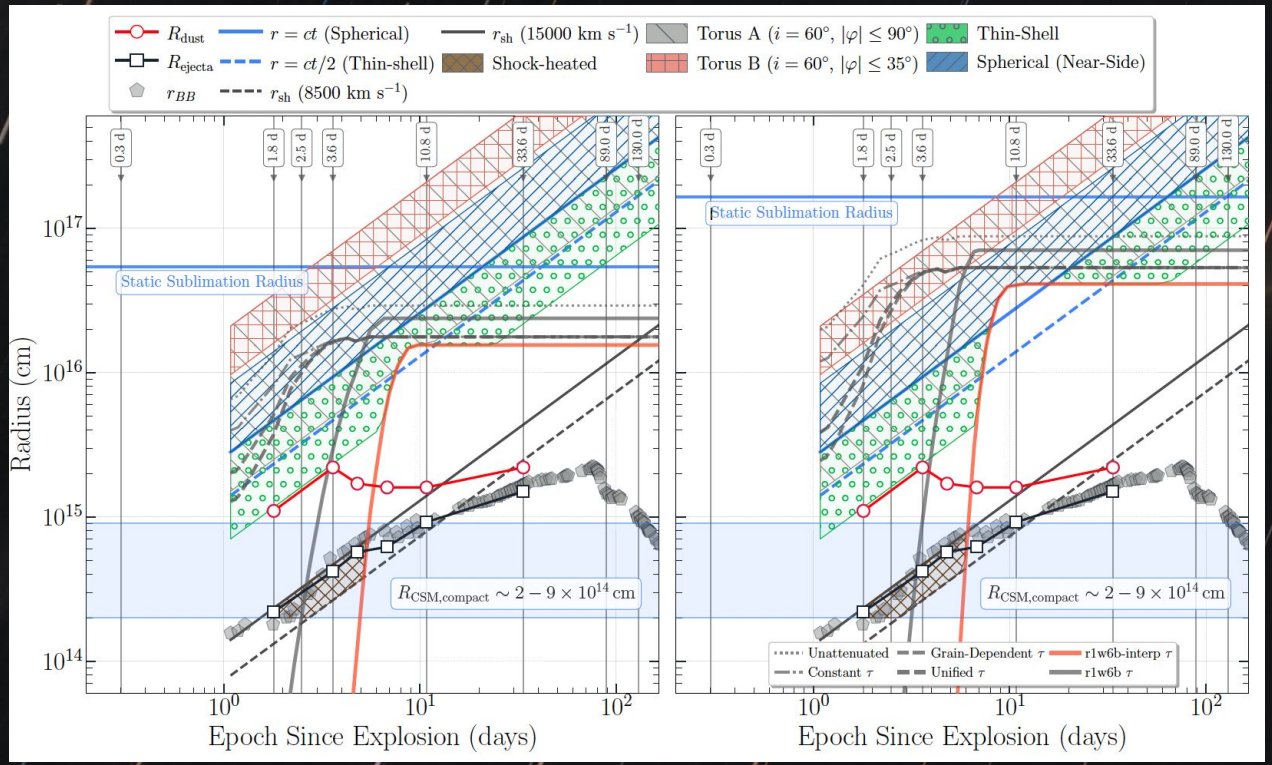

due to a short-lived radiative flash Echo

- from pre-existing dust at 1e15cm, not shock-heated or newly formed dust.
- Requires high optical depth CSM so that dust grains at 1e15cm can survive.
- Time-dependent sublimation and attenuation imply a partially evacuated dust-free cavity with outer edge at 1e17 cm, carved by the SN flash in a dense inner wind.
- Geometry + polarization favour a clumpy, equatorially enhanced torus or fragmented ring with a small effective covering fraction. IR excess resulted from a near-side flash echo.

Late IR Echo

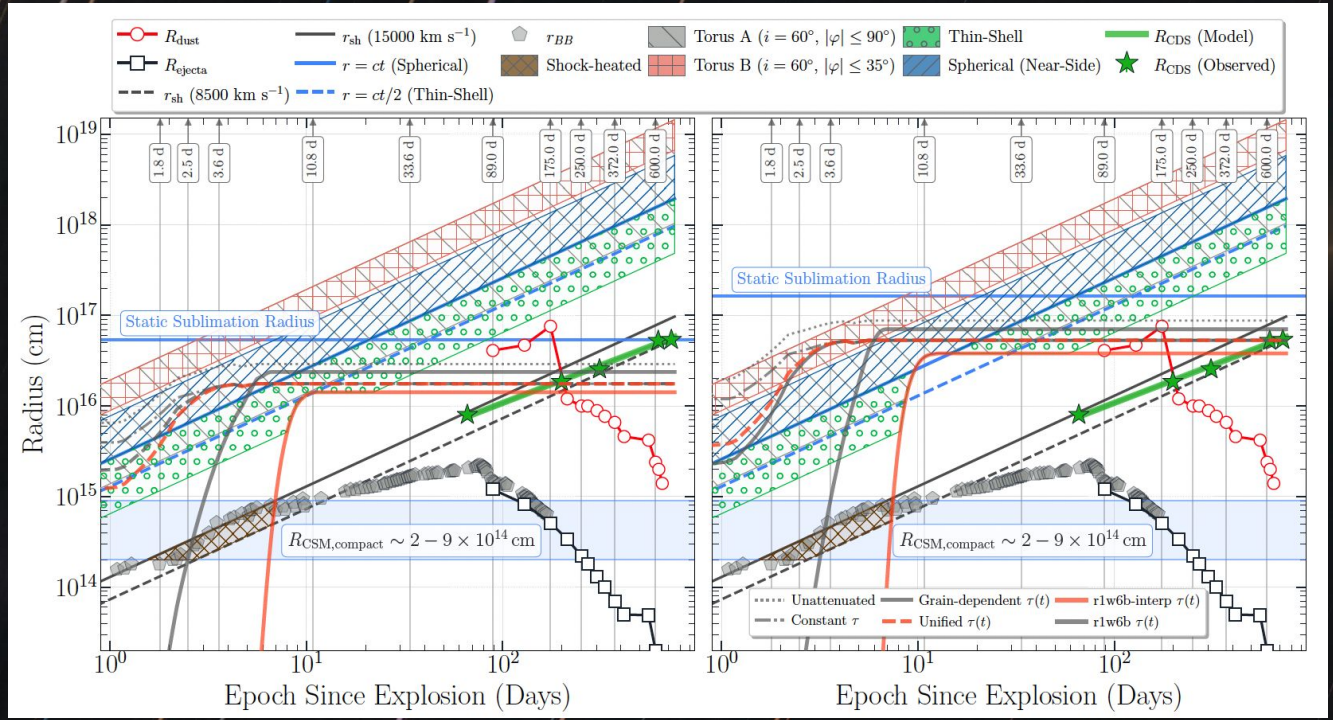

Late Echo and Onset of New Dust

- A broader IR rebrightening at >90 d arises from a **delayed echo in an extended CSM** at 1e16 cm, well beyond the CDS and forward shock.
- The IR blackbody radii rule out shock-heated dust and CDS dust as the dominant source before 175 d.
- Post 175d, the BB radii falls within the CDS/ejecta radius and is consistent with IR excess from newly formed dust in the CDS/Eejecta.

Halpha Modelling

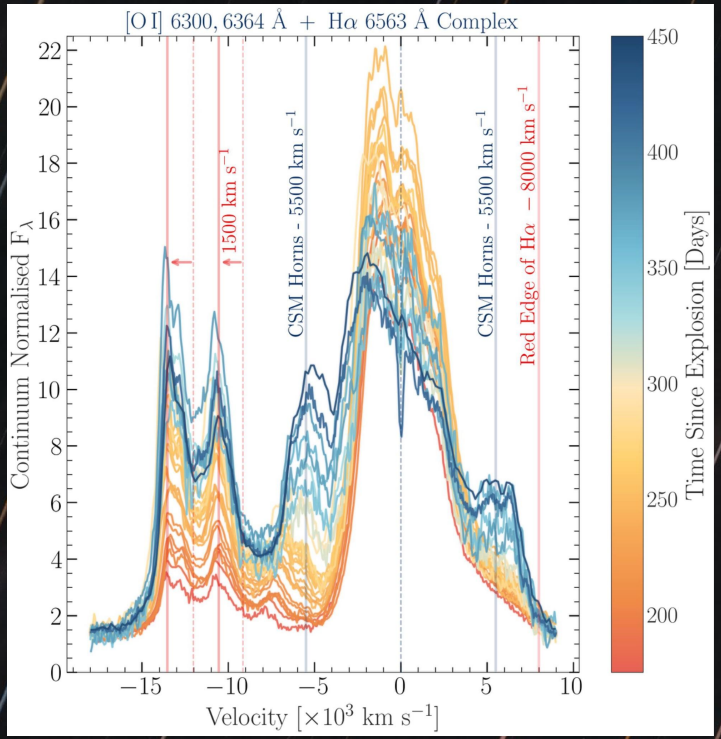

We model the redward attenuated emission line profile of Halpha with time to infer dust properties.

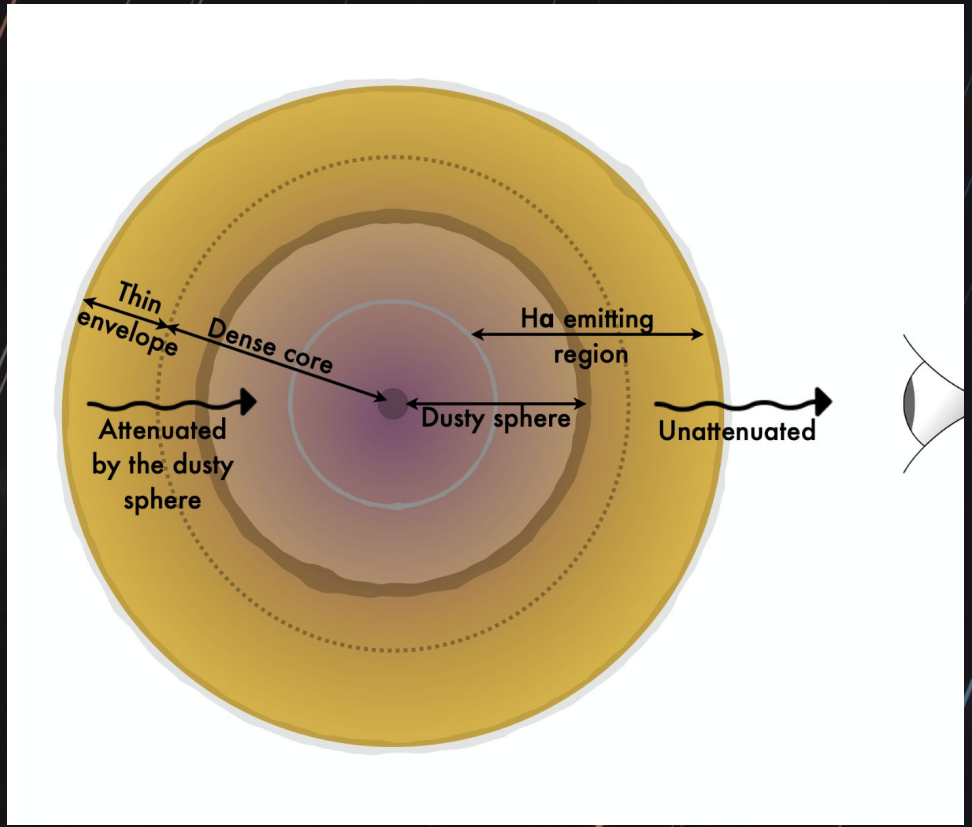

We assume a spherical ejecta with a flat-density core and steep outer envelope, and adopt only silicate dust to avoid composition degeneracies.

Halpha Modelling

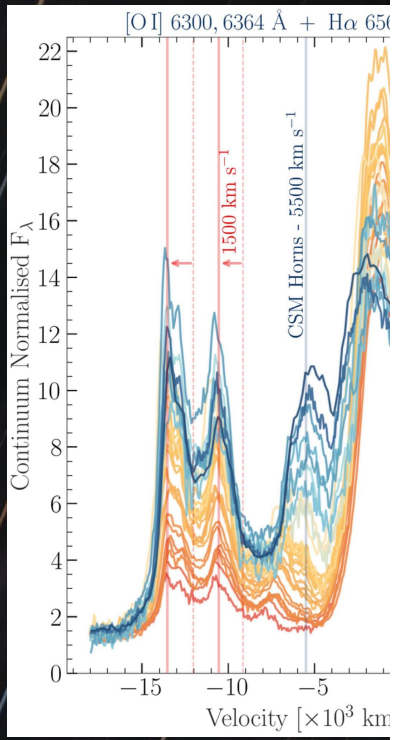

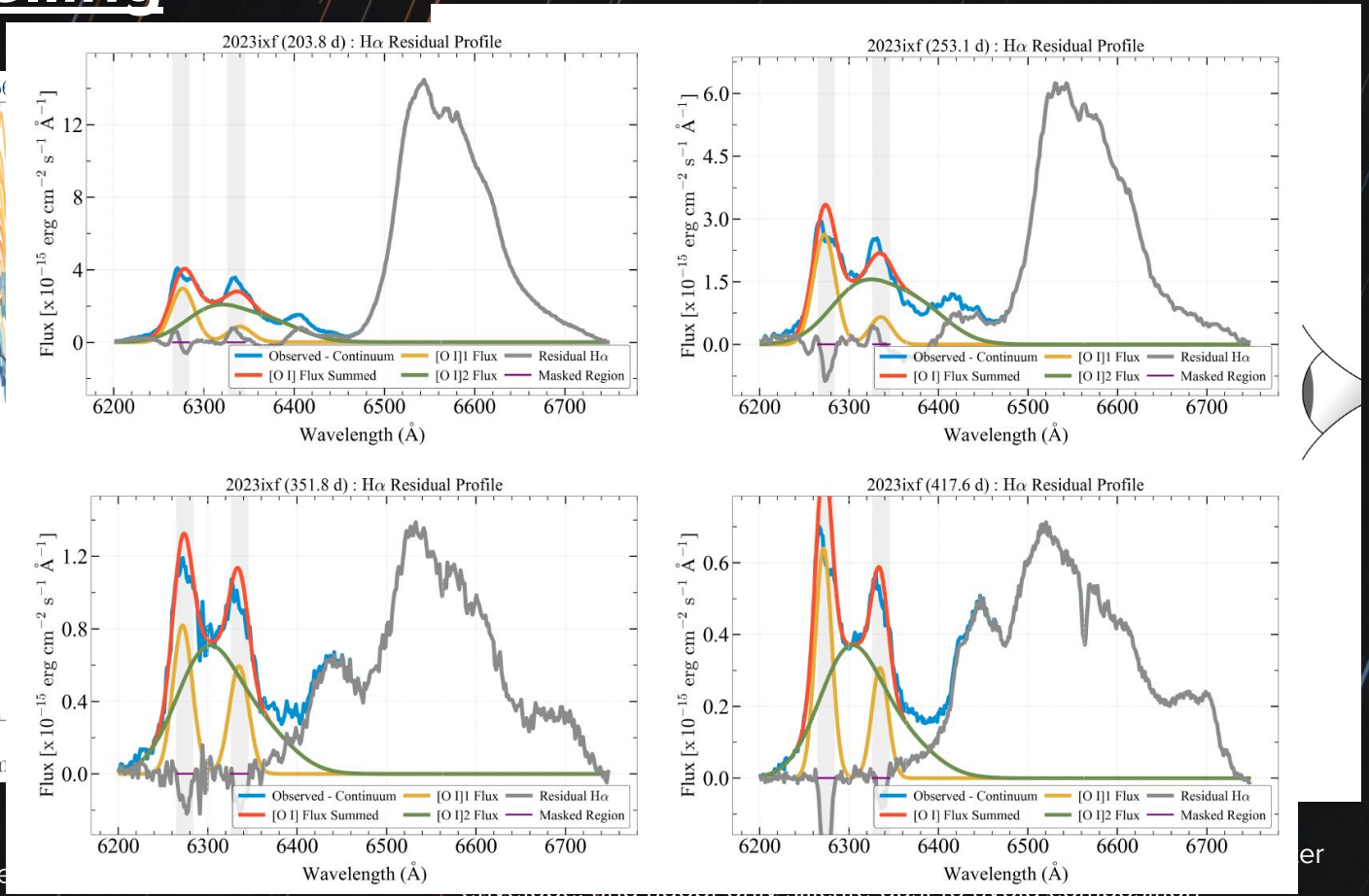

We model the redward atte
profile of Halpha with time to infer dust properties.

er
degeneracies.

Halpha Modelling

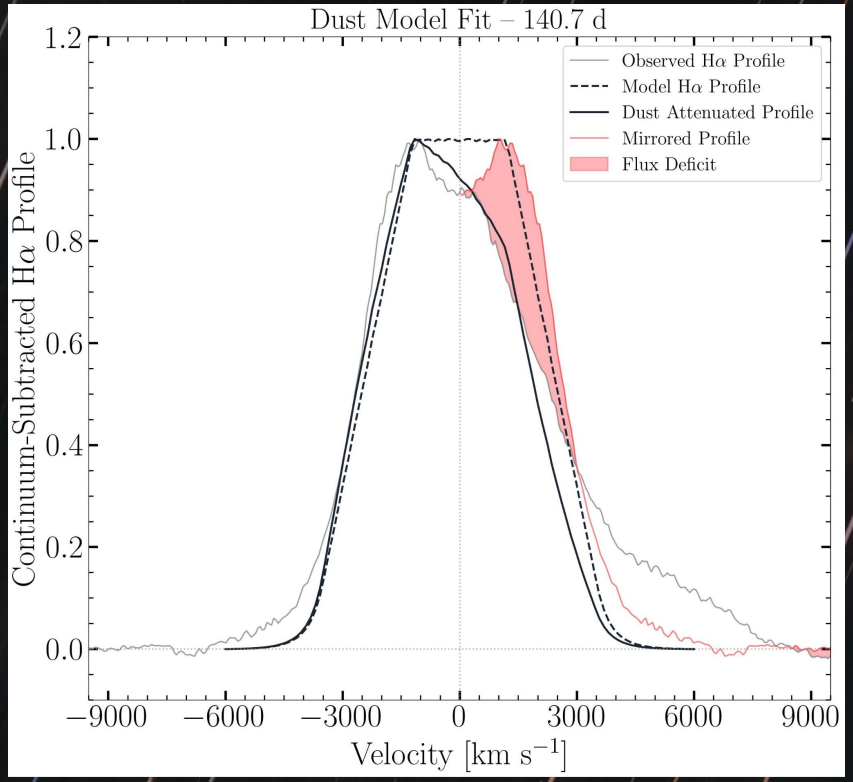

We reconstructed a symmetric Hα profile from the blue wing, then apply dust attenuation to match the observed asymmetric profile.

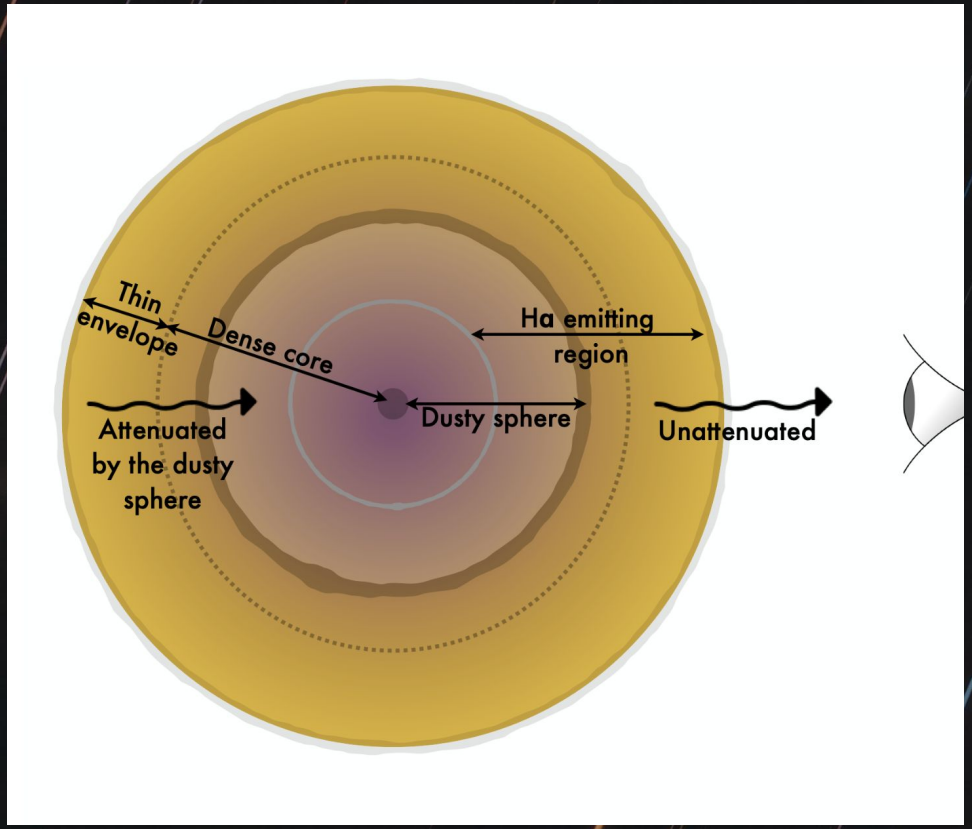

We assume a spherical ejecta with a flat-density core and steep outer envelope, and adopt only silicate dust to avoid composition degeneracies.

Halpha Modelling

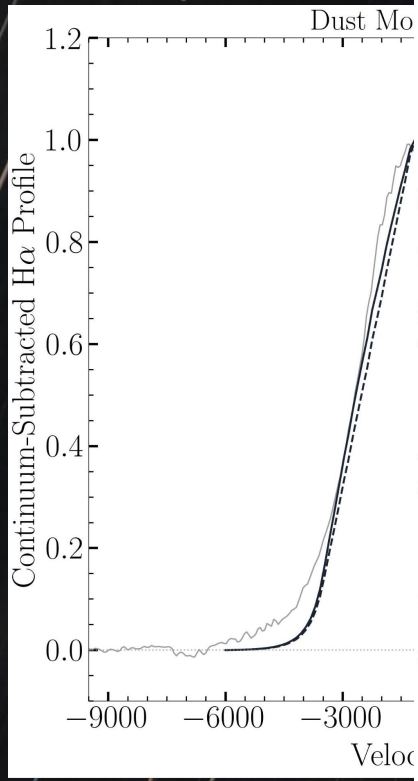

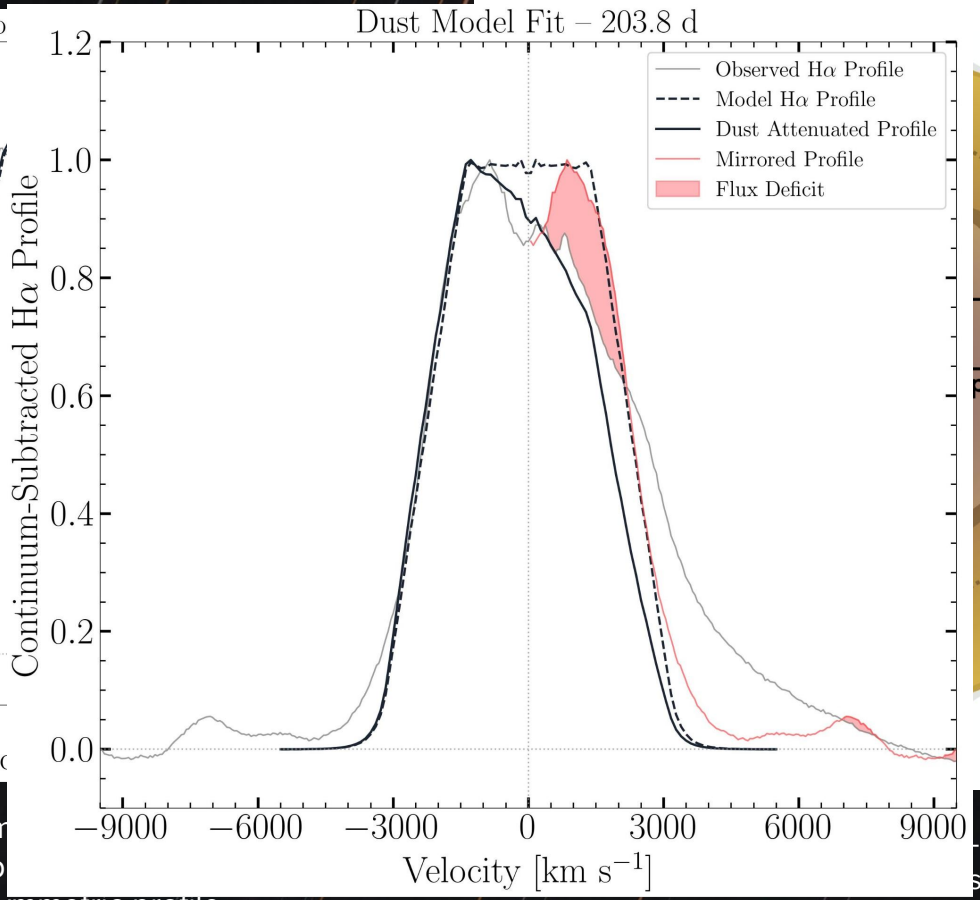

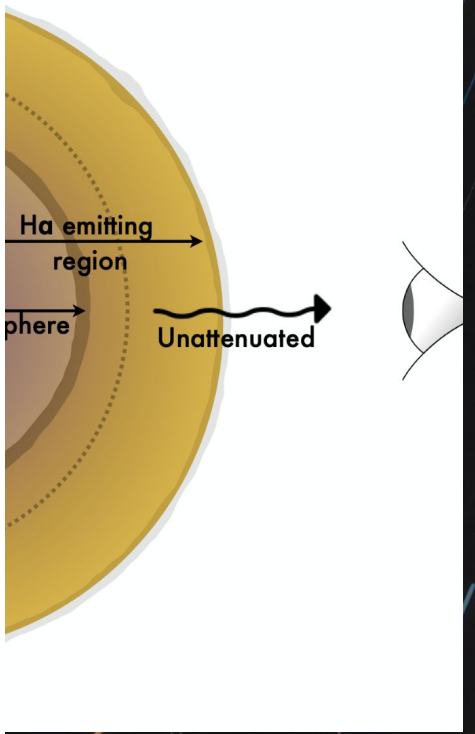

We reconstructed a sym
the blue wing, then app
match the observed asymmetric profile.

-density core and steep outer
st to avoid composition
degeneracies.

Halpha Modelling

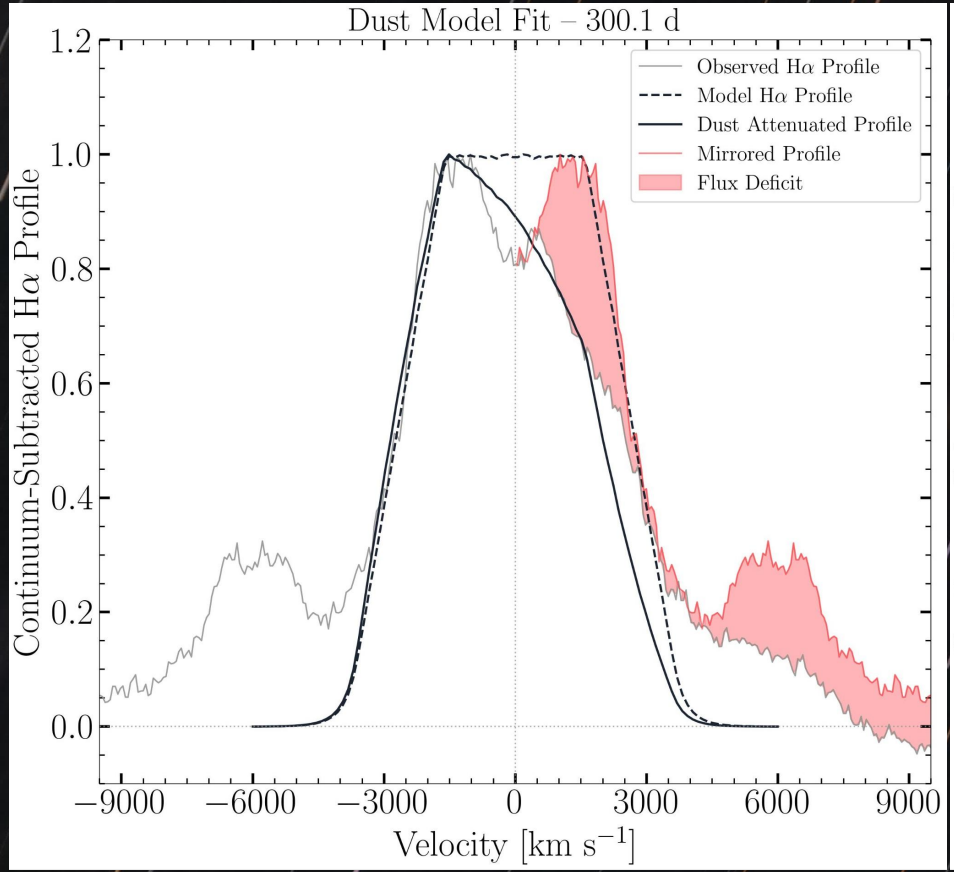

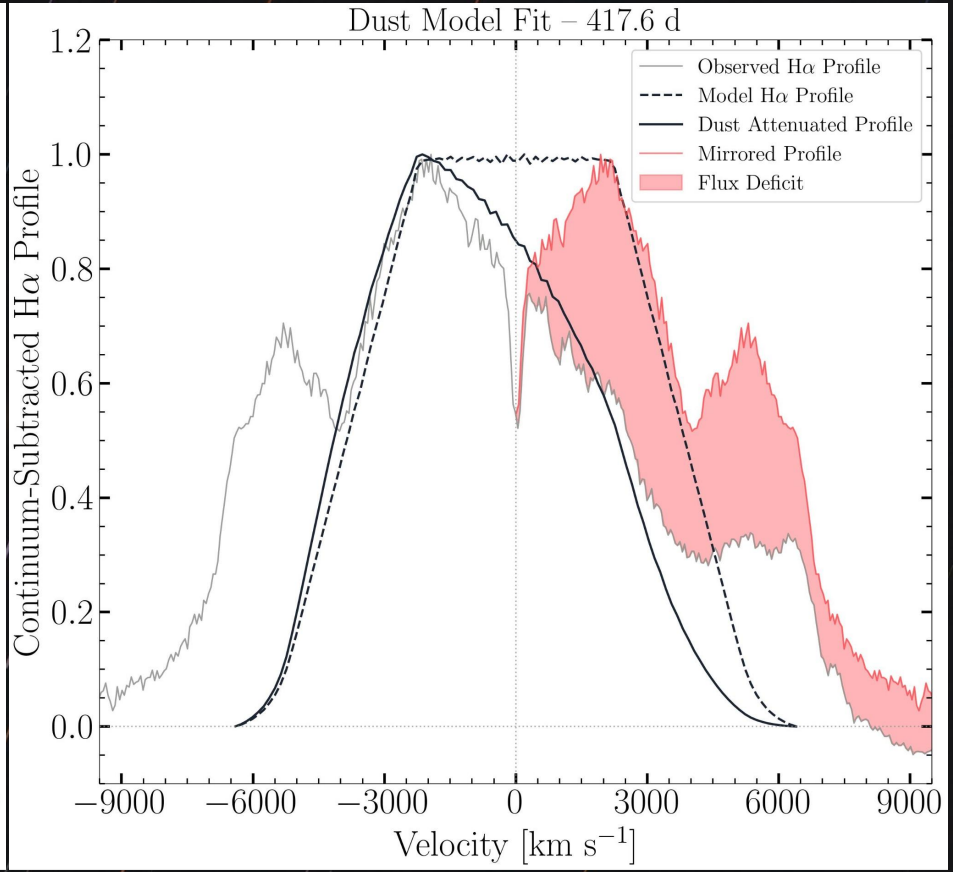

Halpha Modelling

Alternate compositions will scale opacity and hence the inferred dust mass

Day	v_c	$v_{in}(H\alpha)$	v_d	m_d
	10^3 km s^{-1}	10^3 km s^{-1}	10^3 km s^{-1}	10^{-5} M$_\odot$
140	3.5	1.2	3.1	0.15
204	3.1	1.4	3.0	0.26
300	3.6	1.6	3.5	1.0
418	5.1	2.2	4.4	6.0

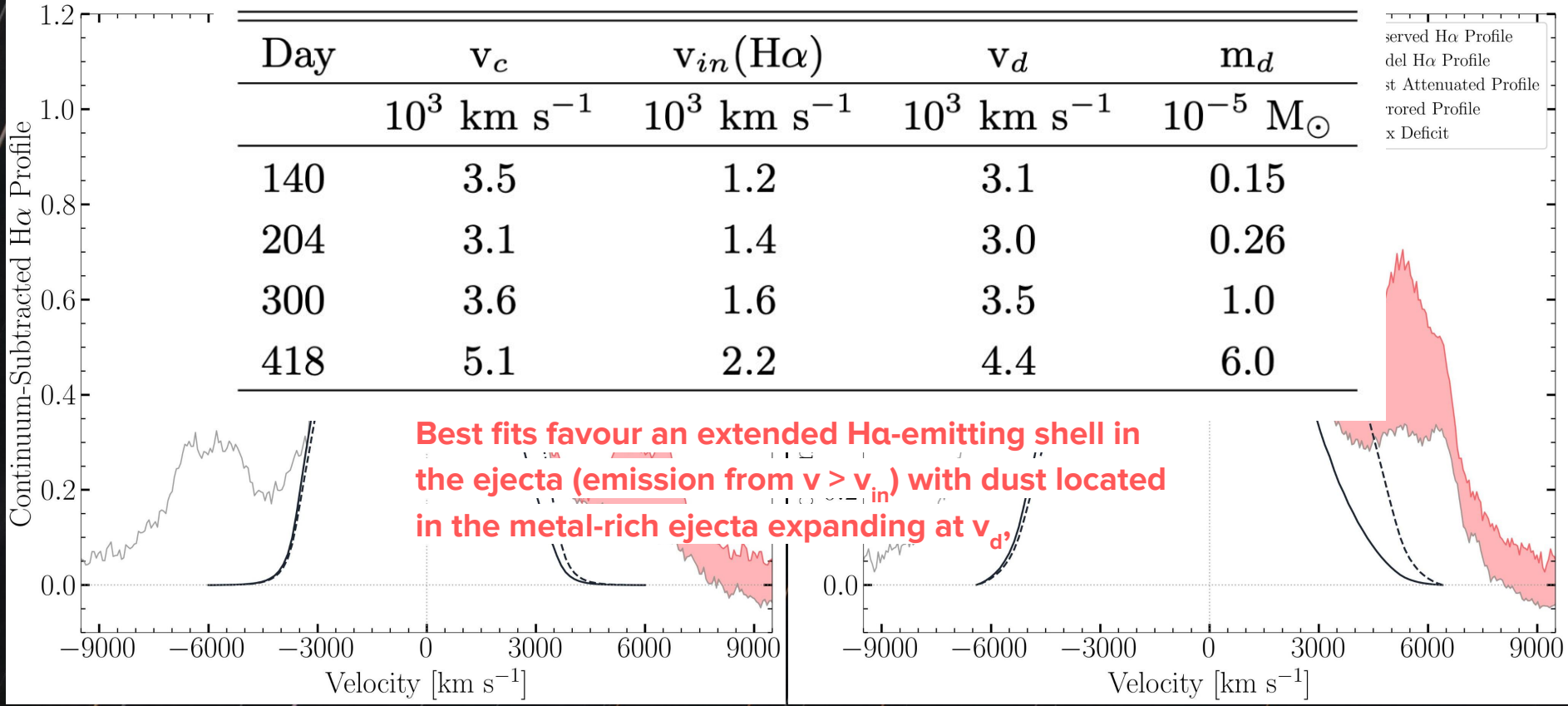

Best fits favour an extended Hα-emitting shell in the ejecta (emission from $v > v_{in}$) with dust located in the metal-rich ejecta expanding at v_d,

Onset of Dust Formation Signatures in Type II SNe

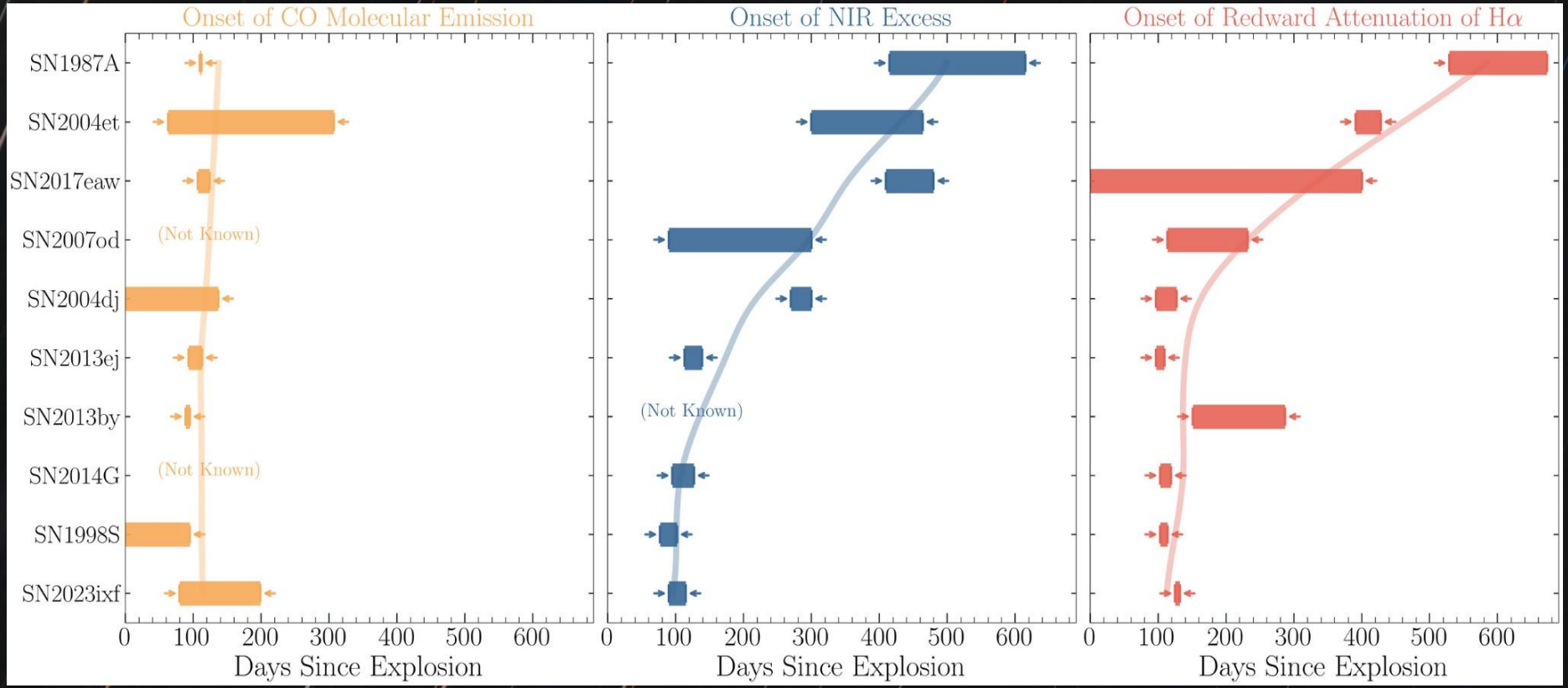

Dust Mass Timeline

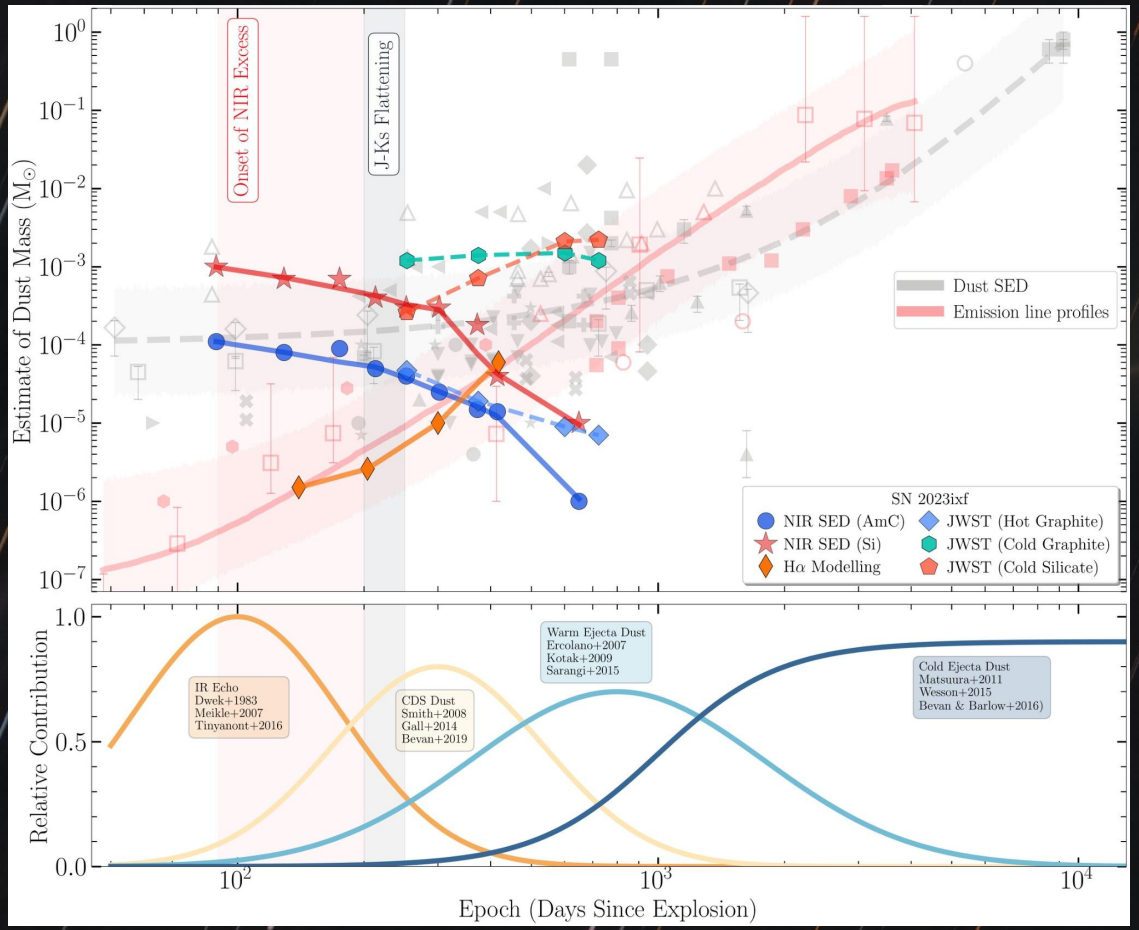

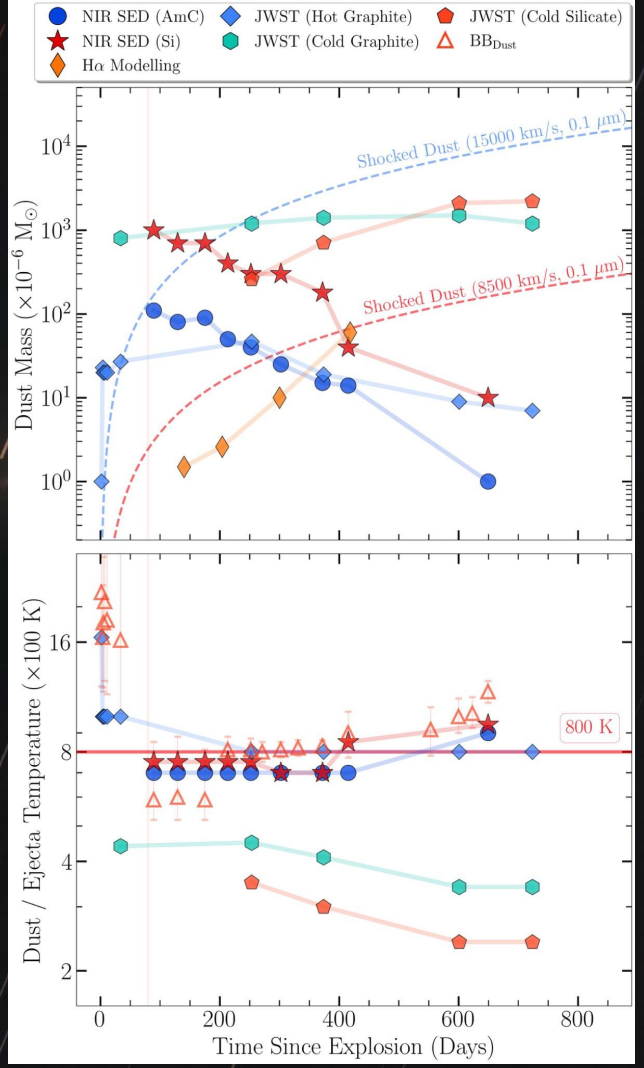

Stabilizing Mass-Temperature Degeneracy

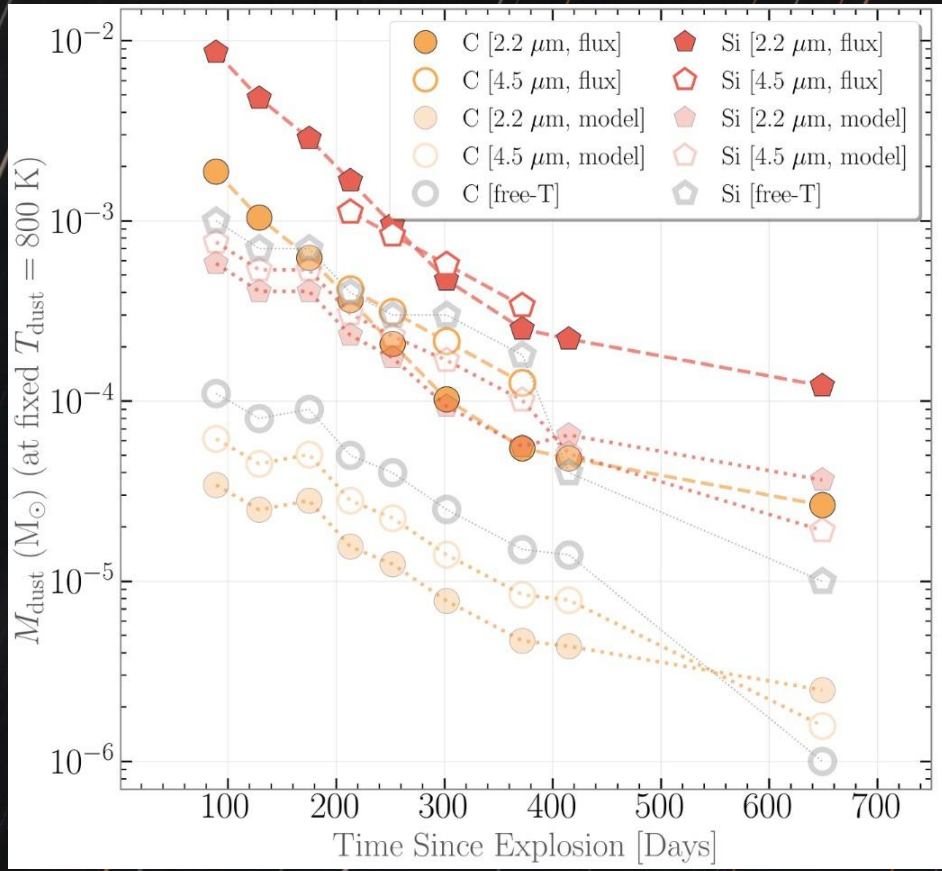

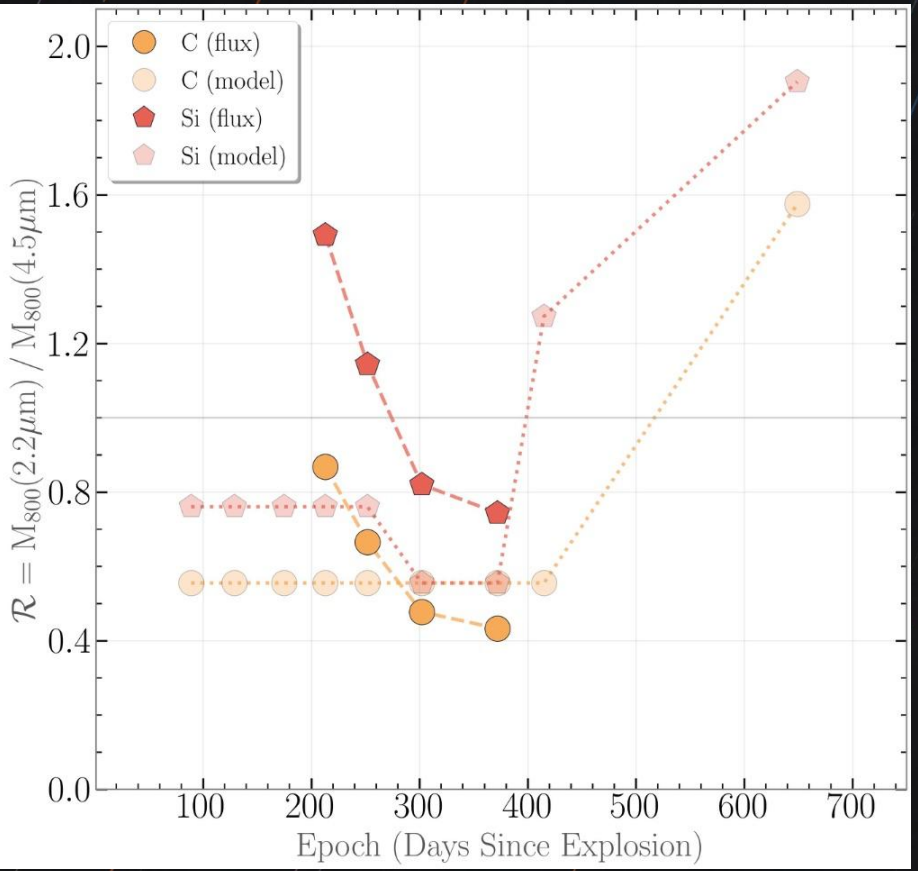

Summary

SN 2023ixf is an exceptionally **nearby Type II SN** and a powerful **laboratory for studying dust and CSM** around Red Supergiants.

- The SN shows a **multi-phase dust evolution** with **early and late IR echoes** and **later CDS/ejecta dust**.
- An early **IR flash echo** (1.8–33.6 d) arises from **pre-existing circumstellar dust (1e15cm)** in a compact inner wind.
- The SN flash carves a **dust-free cavity** within **the aspherical, low-covering-fraction inner CSM** (torus/equatorial-ring).
- A broader **late IR echo** (>90 d) arises from illumination of a more extended **low-density CSM (>1e16cm)**.

- After 130 d, **new dust forms in the CDS** **leading to** growing **Hα red–blue asymmetry** from **increasing dust optical depth** in the line-forming region**, obscuring the receding side** by newly formed dust.
- The Ks-band flattening at around 250d and the steeper attenuation of the **Hα profiles**, indicates **dust formation in the ejecta.**
- The luminosity ratio L_dust/L_ejecta grows from **1% to 100%**, making dust the **main energy channel** by 650 d, and confirming the onset of newly formed dust.

- **Newly formed Dust mass** inferred from SED and line modelling rises from 1e-6 **to** 1e-3 solar mass from 130d to 650d in the **CDS/ejecta**.
- We estimate an illuminated dust mass of 1e-5 solar mass for the early IR echo and around 5e-5 solar mass for the extended IR echo.

Questions Please?

Comet C/2023 ZTF

Nikon Z6 + 2 inch f/4.9 Refractor,
SkyGuider Pro,
Stack of 30s * 85 Frames,
Flat and Dark Corrected